Climate Dynamics (2023) 61:633–667
https://doi.org/10.1007/s00382-022-06590-w

High resolution projections for extreme temperatures and precipitation over Greece

Nadia Politi[1,2] · **D. Vlachogiannis**[1] · **A. Sfetsos**[1] · **P. T. Nastos**[2]

Received: 15 January 2022 / Accepted: 8 November 2022 / Published online: 30 November 2022

Abstract
The present study investigated future temperature and precipitation changes over Greece using the Weather Research and Forecasting (WRF) model. WRF was driven by EC-EARTH over Greece at very high resolution for the historical period (1980–2004), along with projected simulations, in the near future (2025–2049) and far future (2075–2099) under the Representative Concentration Pathways 4.5 (RCP4.5) and 8.5 (RCP8.5). Climatic variables were produced at 5-km grid spacing and 6-h interval. The historical simulation was evaluated against the available station observations. The analysis showed that the model underestimated the maximum temperatures and slightly overestimated the minimum temperatures. Also, the model simulated a small dry bias in precipitation with an excellent representation of the spatial patterns. The model projections for temperature under the two emission scenarios compared to the historical simulation revealed a robust magnitude of future warming with the most pronounced changes predominantly over the eastern areas of the country under the RCP8.5 in the far future. Projected precipitation changes were more evident in the far future with an overall decrease of the annual precipitation all over the eastern part of the country (with islands included) with the most dramatic reductions (above 40%) of seasonal precipitation observed under RCP8.5. Increases in the number of hot days were found everywhere with more pronounced changes over the plain areas under RCP8.5 in the far future. Significant increases of dry days were projected over the eastern part of the mainland and more intensely under RCP8.5 in the far future.

Keywords WRF downscaling · GCM EC-EARTH · High resolution · Climate change · Extreme temperatures · Precipitation · Climate indices

1 Introduction

Climate change is one of the greatest challenges humanity is currently facing. The global average temperature has been rising and projected to increase up to around 2–5 °C by the end of the twenty first century based on different emissions scenarios and socio-economic pathways (Shared Socioeconomic Pathways, SSP) (European Environment Information and Observation Network (Eionet) 2022). Accurate numerical systems for climate simulation and projection at sufficiently high resolution are required for effective climate change mitigation and adaptation, which will improve the resilience of the society.

The two Representative Concentration Pathways (RCP) most frequently used by almost all modeling groups and considered as future greenhouse gas emissions scenarios, are RCP4.5 and RCP8.5. The later RCP8.5, regarded as the most severe scenario, is built on the assumption that the emissions rise throughout the twenty-first century (Riahi et al. 2011) implying at its end a radiative forcing of 8.5 W/m^2 relative to the pre-industrial era. On the other hand, RCP4. scenario is representing an increase of 4.5 W/m^2 in radiative forcing relative to the pre-industrial era. It is a scenario according to which emissions peak around 2049 and stabilize until 2099 by employment of a range of technologies and strategies for reducing greenhouse gas emissions. By the year 2099, the corresponding to RCP4.5 and RCP8.5 greenhouse gas concentrations become equivalent to 650 and more than 1370

✉ Nadia Politi
nadiapol@ipta.demokritos.gr

[1] Environmental Research Laboratory, INRaSTES, NSCR Demokritos, Patr. Gregoriou E' & 27, Neapoleos Str., PO Box 60037, 153 41 Athens, Greece

[2] Laboratory of Climatology and Atmospheric Environment, Faculty of Geology and Geoenvironment, National and Kapodistrian University of Athens, Athens, Greece

parts per million (ppm) carbon dioxide (CO_2), respectively (Moss et al. 2010).

Successive CMIP (Coupled Model Intercomparison Project) initiatives based on GCMs have been able to provide large ensembles that showed some consistent signals of temperature and precipitation over the European region (Cattiaux et al. 2013; Basharin et al. 2015). CMIP3 simulations have preceded with an average grid mesh larger than 2.5° and adopting the SRES emission scenarios (Nakicenovic et al. 2000), while the CMIP5 simulations employed grids with approximately twice finer resolution than in CMIP3 (Lionello and Scarascia 2018). The new generation of Earth system models provides the opportunity to assess the latest ensemble (CMIP6) with much higher climate sensitivity (e.g. Forster et al. 2019) related to the improved representation of clouds and changes in the model physics (Zelinka et al. 2020). Recently, the EUROCORDEX projection ensemble has been enhanced as part of the European Copernicus Climate Change Service (C3S), resulting in a high resolution (0.11 degrees) ensemble of unprecedented size (Jacob et al. 2020). A high RCM resolution helps to better represent topographic effects, can potentially help to reduce model uncertainties and improve precipitation simulations (Hawkins and Sutton 2009; Sylla et al. 2009; Cardoso et al. 2013, 2019; Warrach-Sagi et al. 2013; Torma et al. 2015; Warscher et al. 2019; Tian et al. 2020; Politi et al. 2021). Other studies have indicated improved description of simulation results regarding temperature and its extremes (Soares et al. 2012; Berg et al. 2013; Pérez et al. 2014; Gao et al. 2015; García-Valdecasas Ojeda et al. 2015; Kryza et al. 2017; Lyra et al. 2018).

Projected changes in the seasonal variability of temperature and precipitation for the region support the characterization of the Mediterranean as one of the most prominent global climate change hot spots (Giorgi 2006; Diffenbaugh and Giorgi 2012; Zittis et al. 2019; Feyen et al. 2020). The Mediterranean Basin, located in a transition zone between mid-latitude and subtropical atmospheric circulation regimes, with large topographic gradients, is very sensitive to changes in the global mean climate state. Research studies based on the physical processes related to projecting future changes (Giorgi and Lionello 2008; Mariotti and Dell'Aquila 2012; Barcikowska et al. 2018; Lionello and Scarascia 2018) found that the important factors that influence the response of the future regional atmospheric circulation and are responsible for the effect of global warming are the increase of barotropic sea-level pressure (with NAO climate variability) and geopotential height at the 500 hPa level in the central Mediterranean, along with the thermal inertia of the large water mass of the Mediterranean Sea among continents at these latitudes. The increasing anticyclonic circulation over the region would lead to a reduction of precipitation over most parts of the region, and intensification at sub-regional scale in the northwestern areas. On the other hand, during summer, the circulation change is associated to the intensification of the Azores anticyclone (reduction of weather regimes producing precipitation events in the northern part of the basin) and increased advection of warm dry continental air masses towards the central and eastern Mediterranean. Also, NAO variability associated with high positive values explains (in winter) up to 30% of the decadal precipitation changes in the Mediterranean region.

As a Mediterranean country, Greece is highly vulnerable to the impact of climate change (Barros 2014). The first comprehensive climate impact study was published in 2011 by an interdisciplinary committee set up by the Bank of Greece. According to the findings of this report, based on the two extreme climate change scenarios B2 and A2 of IPCC Working Group III, it is expected that by the end of the twenty-first century, the decrease in precipitation levels due to anthropogenic factors would range between 5% and roughly 19% countrywide, depending on the scenario, while mean temperature would increase by 3.0–4.5 °C, respectively. Heavy rainfall is projected to become more frequent in eastern and central Greece and in northwestern Macedonia, while drought would increase for the eastern mainland and northern Crete (Zerefos et al. 2011). Previous studies, that analysed the potential seasonal (winter and summer) future changes in temperature and precipitation conditions over the Greek area, were conducted by Tolika and Zanis (2012) during PRUDENCE and ENSEMBLES projects, but in coarse resolution (50–25 km, respectively). More specifically, the warming during winter was in range of about 2.5–4.5 °C and generally it increased from the coastal areas to the central and northern continental interiors based on the scenarios. The warming was even higher during summer with an increase from 3.5 to 6 °C. Tolika and Zanis (2012) and Maheras et al. (2008) also noted that Greece would experience a persisting absence of rainfall. Winters were estimated to be drier by the end of the twenty-first century with a decrease up to − 30% in southern Greece, while the expected changes of summer precipitation showed a prevailing decrease or rainfall heights up to − 60% with respect to the reference period (mainly in the areas of Peloponnese and eastern Aegean Sea). According to Giannakopoulos et al. (2011) for IPCC SRES A1B scenario during the midcentury period, the largest increases were found in 'summer' days (> 25 °C) and 'tropical' nights (> 20 °C), while urban areas would face warmer temperatures, which was translated into more days with maximum temperature above 35 °C. The increase was also found to be greater in summer maximum temperatures compared with the winter minimum temperatures. Kostopoulou et al. (2014) also estimated that the warmer future of the area would also include a strong increase in the occurrence of tropical nights, summer and hot days and decrease of frost days and wet days

based on the SRES A1B for the late century. Finally, a number of research works have contributed to the investigation of climate change in Greece, using RCPs scenarios, mostly in the country's specific areas and not necessarily at high resolution. Their studies are dealing with the research over different sectors that climate change affects such as: drought and land degradation [e.g. (Anagnostopoulou 2017; Kairis et al. 2022)], forest fires [e.g. (Varela et al. 2020; Rovithakis et al. 2022)], climate parameters and índices [e.g. (van der Schriek et al. 2020; Georgoulias et al. 2022)], human health and tourism [e.g. (Nastos et al., 2019; Katavoutas et al. 2021)], energy sector [e.g. (Katopodis et al. 2019; Droutsa et al. 2021)].

Thus, given the country's vulnerability, the need for updated and reliable information on climate change projections based on more recent IPCC emission scenarios and higher resolution data for the country is profound. The geomorphological complexity of Greece (mostly mountainous country with an extended coastal line and scattered islands) enhances the need for very high-resolution climatology studies. These topographic features influence the local climate characteristics of parts of the country, providing many different climatic variations across it (Eleftheriou et al. 2018). Taking also into consideration (1) the lack of reliable observational gridded dataset covering the entire country which is mandatory for fine resolution studies (1–4 km) in case of convection-permitting models, (2) computational cost and storage, the high horizontal resolution of 5-km used in our study, produces high-resolution climate information that is computationally affordable and suitable for climate impacts/services applications that require high-scale climate information for Greece.

This work is linked to our previous recent studies, which successfully established confidence in the use of dynamically downscaled simulations with WRF model using GCM historical and future datasets to explore the climate change signal at high resolution for Greece. More specifically, these studies (Politi et al. 2017, 2018, 2020, 2021; Katopodis et al. 2020, 2021) included extensive analysis of sensitivity tests of physics parameterization schemes, initialization times, and domain resolutions investigating the performance of the WRF model to dynamically downscale the coarse-resolution ERA-Interim dataset to the high spatial resolution of 5 km grid over the study area. It is worth also mentioning that other relevant studies have indicated improved description of simulation results using the WRF model, clearly supporting its use as a regional climate model (Soares et al. 2012; Berg et al. 2013; Wagner et al. 2013; Gao et al. 2015; García-Valdecasas Ojeda et al. 2015; Prein et al. 2016; Sun et al. 2016; Komurcu et al. 2018; Garrido et al. 2020; Ban et al. 2021).

The aim of this study is to investigate climate change effects in temperature (TX and TN) and precipitation (RR) fields with future projections at very high spatial resolution in Greece. To our knowledge, the extended high-resolution datasets derived for the region by downscaling EC-EARTH GCM data to 5 km for Greece are unique so far. The focus of this paper is on climate change projections for Greece of the high resolution fine nest simulations of TX, TN and RR. The details of the applied methodology are described in Sect. 2, including the various steps for the model setup and statistical analysis performed, along with a description of the observational data. Sections 3 and 4 present the analysis and discussion of the results concerning the evaluation of the performance of the downscaled outputs during the historical period and the estimated future changes in temperature and precipitation fields and their extremes under the two RCPs. Section 5 summarizes the results with some concluding remarks and key findings.

2 Models, data and methods

Future changes in precipitation and temperatures have been examined by comparing the projections from the WRF simulations with the control run through the Delta-change approach (Hay et al. 2000). A 2-tailed t-test was also used to diagnose the statistical significance of the projected changes.

2.1 Global climate model

The selected GCM for our study was the EC-Earth model which is a full physics seamless atmosphere–ocean sea- ice coupled earth system prediction model (Hazeleger et al. 2010) developed from the operational Integrated Forecast System (IFS) cycle 31r of ECMWF. EC-Earth model has been incorporated in CMIP5 and more recently in CMIP6

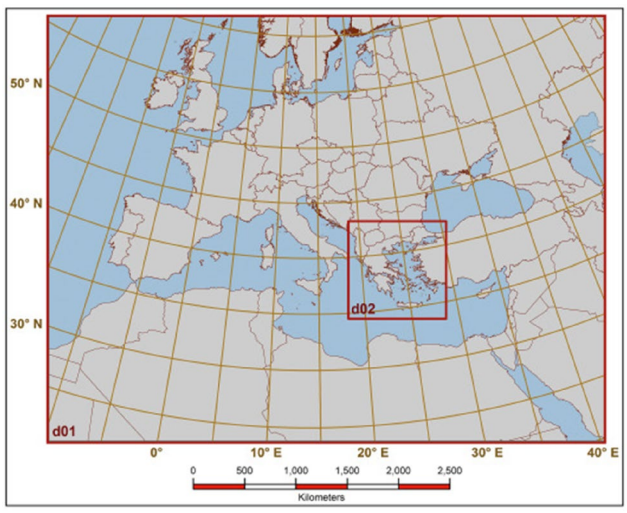

Fig. 1 Modelling domains: D01 (outermost domain) 20 km resolution and d02 (nested domain, region of Greece) 5 km resolution

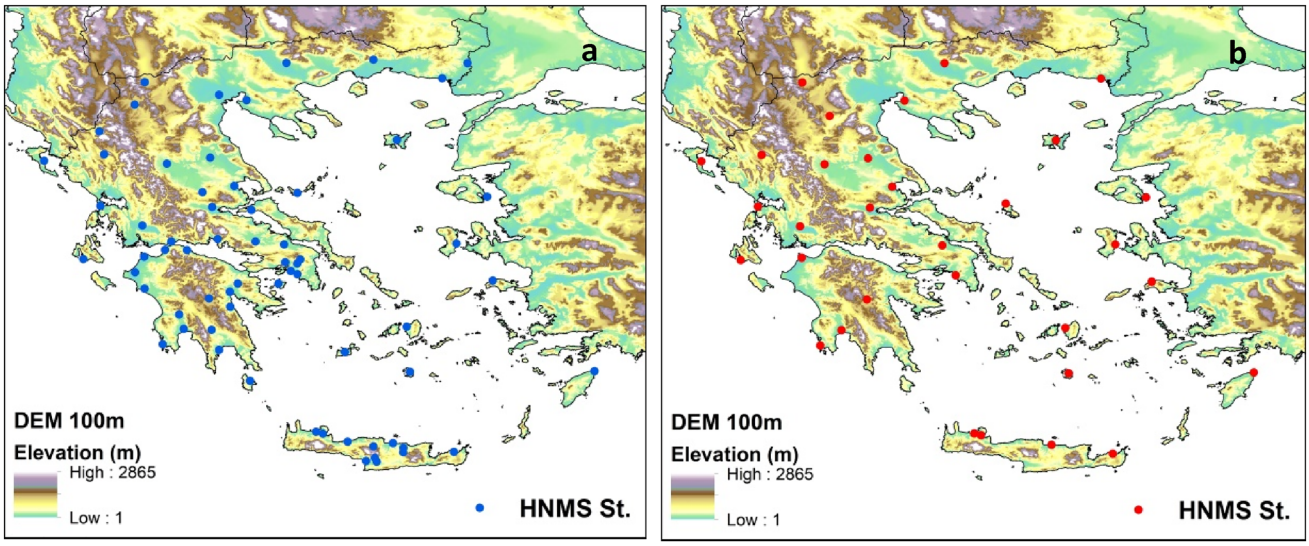

Fig. 2 The observational stations used for the validation of the model results: **a** precipitation (blue dots) and **b** temperature (red dots)

Table 1 Summary of statistical formulas calculated for model evaluation in this study:

Parameter	Formula	Range	Ideal value
Mean bias error	$BIAS = \frac{1}{N}\sum_{i=0}^{n}\left(f_i - o_i\right) = \bar{f} - \bar{o}$	$(-\infty,\infty)$	0
Root mean square error	$RMSE = \sqrt{\frac{\sum_{i=0}^{n}(f-o)^2}{N}}$	$(0,\infty)$	0
Mean absolute error	$MAE = \frac{1}{N}\sum_{i=0}^{n}\left\|f_i - o_i\right\|$	$(0,\infty)$	0
Pearson correlation coefficient	$COR = \frac{\sum_{i=1}^{n}\left(f_i-\bar{f}\right)(o_i-\bar{o})}{\sqrt{\sum_{i=0}^{n}\left(f_i-\bar{f}\right)^2}\sqrt{\sum_{i=0}^{n}(o_i-\bar{o})^2}}$	$(-1,1)$	1
Modified Index of Agreement	$MIA = 1 - \frac{\sum_{i=1}^{n}\left\|(o_i-f_i)\right\|}{\sum_{i=1}^{n}\left\|(f_i-\bar{o})\right\|+\sum_{i=1}^{n}\left\|(o_i-\bar{o})\right\|}$	(0,1)	1
Nash–Sutcliffe efficiency	$NSE = 1 - \frac{\sum_{i=1}^{n}(o_i-f_i)^2}{\sum_{i=1}^{n}(o_i-\bar{o})^2}$	(− Inf,1)	1

(Vautard et al. 2021). EC-Earth climate simulations and projections have been widely used for climate studies. In global scale, Hazeleger et al. (2010) indicated that the EC-Earth model demonstrates very good forecasting skill from daily up to interannual time scales (interannual variability must be well represented for successful seasonal-to-decadal predictions) and for long-term mean climate. Hazeleger et al. (2013) has shown that the EC-Earth model simulates well the tropospheric fields and the dynamic variables, but not as good the surface temperature and fluxes. More recently, the model was also downscaled to regional scale in the Framework of Coordinated Regional Downscaling Experiment (CORDEX) over different CORDEX domains at a spatial resolution of 50 km and 12 km (e.g. Jacob et al. 2014; Prein et al. 2016). Soares et al. (2017) and Cardoso et al. (2019) denoted that WRF at 9-km high resolution driven by EC-Earth results were in good agreement with EUROCORDEX and observational data for Portugal.

The set-up of the atmospheric model in the EC-Earth version 2.3 corresponds to the use of a horizontal spectral resolution of T159 (triangular truncation at wavenumber 159), roughly 125 km, and a vertical grid with vertical 62 levels of a terrain-following mixed sigma-pressure hybrid coordinates, of which about 15 are within the planetary boundary layer (PBL).

2.2 Model setup

We perform regional climate simulations for the area of Greece with the non-hydrostatic Weather Research and Forecasting model (WRF/ARW, v3.6.1) (Skamarock

Table 2 Definition of extreme temperature and precipitation indices

Code	Name	Definition	Unit
SU	Summer days	Annual count when daily maximum temperature > 25 °C	Days
HD	Hot days	Annual count when daily maximum temperature > 35 °C	Days
TR	Tropical nights	Annual count when daily minimum temperature > 20 °C	Days
FD	Frost days	Annual count when daily minimum temperature < 0 °C	Days
R20 mm	Very heavy precipitation days	Annual count when precipitation ≥ 20 mm	Days
R50 mm	Extreme precipitation days	Annual count when precipitation ≥ 50 mm	Days
CDD	Dry days	Maximum number of consecutive days when precipitation < 1 mm	Days

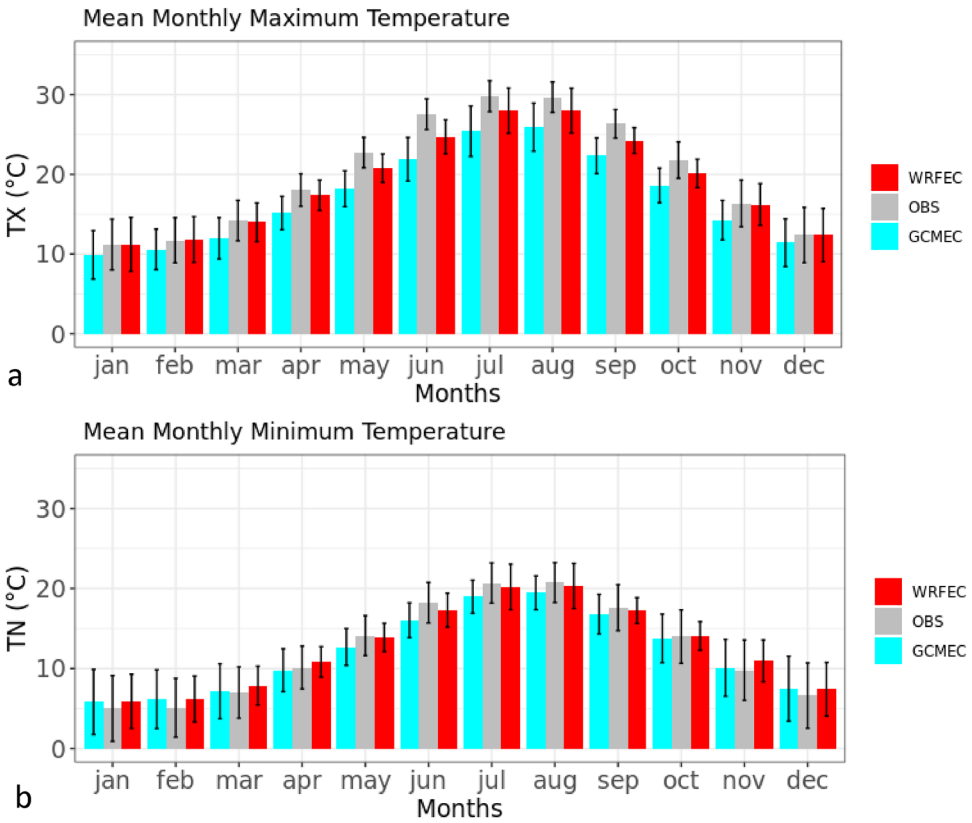

Fig. 3 Mean annual cycle of **a** TX and **b** TN averaged over the historical period of 1980–2004 for the total number of stations for GCMEC, WRFEC and OBS

et al. 2008) in a one-way nesting setup (Fig. 1) with two domains. The first domain (d01) of 20 km resolution is centered in the Mediterranean basin at 42.5 N and 16.00 E, and a second nested domain of 5 km in the area of Greece (d02). The coordinates (LAT, LONG) of the two domains are the following: d01[1]:[UL(33.673, 28.521), UR(41.994, 30.303], LR(42.905, 18.827), LL(34.455, 18.469)] and d02: [UL(54.103, − 27.400), UR(54.103, 59.400], LR(21.004, 40.494), LL(21.004, − 8.494)]. The large-scale circulation in the 20 km domain is nudged towards the forcing boundary conditions with spectral nudging.

The model setup has the following physics options: the Mellor–Yamada–Janjic scheme (MYJ) (Mellor and Yamada 1982) for the planetary boundary layer (PBL) scheme, the WRF single-moment six-class scheme (WSM-6) for cloud microphysics and Betts–Miller–Janjić scheme (Janjić 2001) for the cumulus parameterization. The Rapid Radiative Transfer Model, RRTMG (Iacono et al. 2008), for both longwave and shortwave radiation and finally, the Noah LSM was employed as the land surface model. The boundary conditions for the climate change assessment derive from EC-EARTH climate simulations for RCP 4.5 and RCP8.5 scenario and encompass time slices representative of the historical (1980–2004), midcentury (2025–2049), and end of century (2075–2099) periods. For the future projections,

[1] UP: upper left corner, UR: up right corner, LR: low right corner, LL: low left corner.

the equivalent-CO2 concentration was updated every year accordingly to the emission scenario in the WRF simulations. The downscaling of EC-EARTH historical products (hereafter WRFEC) is carried out in this study under an identical configuration (spatial/temporal resolutions, integrating time step, physics schemes, etc.) with ERA-Interim reanalysis datasets, except of future projections where nudging was not applied.

2.3 Observations

For the comparison of model output data against observed data, the present study focused on model evaluation against real points and only validated observations by the formal meteorological organization of Greece, the Hellenic National Meteorological Service (HNMS). The reason is that the only available gridded observational dataset E-OBS is derived from a very coarse network density for Greece, thus becomes less reliable (Hofstra et al. 2010) for this region which is characterized by complex terrain. The HNMS validated temperature dataset covered the period of 1980–2004 with measurements from 32 stations. On the other hand, the HNMS network of 66 stations provided continuous precipitation observations for the period of 1980–2000. Thus, the model assessment was realized during these specific time ranges as dictated by the validated data availability. Figure 2 illustrates the spatial distribution of the HNMS stations for (a) precipitation and (b) minimum and maximum temperatures. The geographical distribution of the available observational stations reveals, also, the limited number of

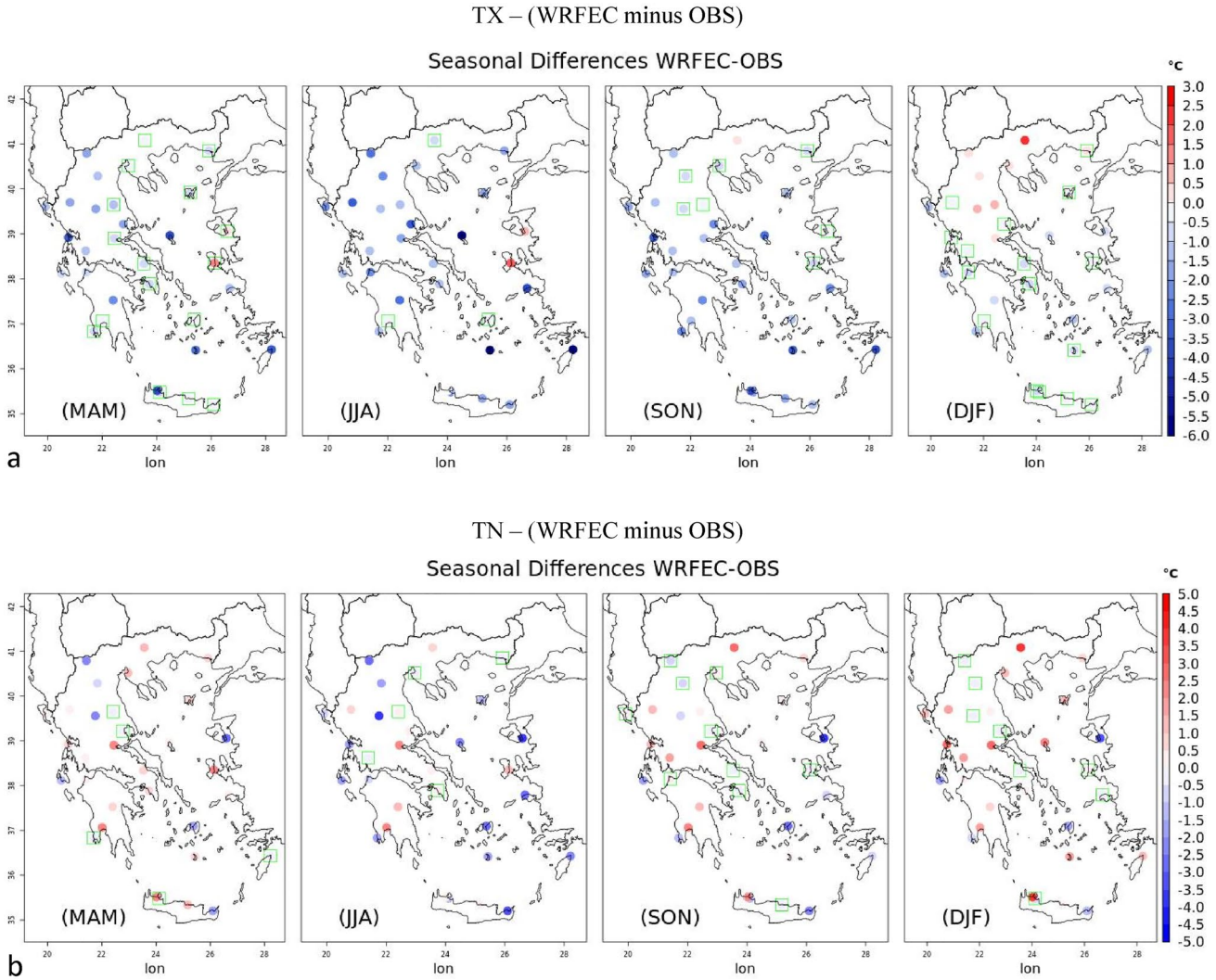

Fig. 4 Differences of mean seasonal **a** maximum and **b** minimum temperatures between WRFEC Control Run (1980–2004) and station observations, (green square points specify no statistical differences between the mean distributions of seasonal TX/TN according to Student's t test at the 95% confidence level)

Table 3 Statistical errors of maximum and minimum temperatures and precipitation model results against observations for all grid points of available stations

TX		COR	BIAS (°C)	RMSE (°C)	MAE (°C)	NSE	MIA
WRCEC	Monthly	0.80	− 1.13	2.99	2.35	0.83	0.80
	Seasonal	0.95	− 1.14	2.37	1.78	0.88	0.82
	Annual	0.65	− 1.14	1.77	1.38	− 0.37	0.5
GCMEC	Monthly	0.92	− 2.98	4.17	3.49	0.67	0.71
	Seasonal	0.94	− 2.97	3.78	3.21	0.67	0.69
TN	Annual	0.41	− 2.98	3.33	3.06	− 4	0.27
WRCEC	Monthly	0.92	0.24	2.57	2.04	0.85	0.81
	Seasonal	0.94	0.24	2.08	1.66	0.88	0.83
	Annual	0.83	0.23	1.6	1.26	0.67	0.72
GCMEC	Monthly	0.87	− 0.42	3.36	2.61	0.73	0.76
	Seasonal	0.87	− 0.42	3.07	2.38	0.74	0.76
RR	Annual	0.75	− 0.42	2.76	2.02	0.10	0.76
WRFEC	Monthly	0.41	− 10.2	64.92	40.31	− 0.16	0.54
	Seasonal	0.57	− 10	120.71	81.78	0.13	0.59
	Annual	0.39	2.9	292	212	− 0.2	0.47
GCMEC	Monthly	0.34	14.3	66.78	41.59	− 0.12	0.40
	Seasonal	0.49	14.2	133.17	89.83	0.2	0.45
	Annual	0.17	14.2	299.02	235.42	− 0.34	0.36

measurements over mountainous, mainland areas that might disrupt the evaluation process over such regions.

2.4 Statistical analysis

The model quality assessment is focused on the capacity of the WRFEC of the inner (nested) domain historical runs to correctly represent the spatial and temporal structures of the mean variables and their probability distributions. The approach involved the comparison with the available observational data for the historical period. WRF downscaled results were converted to daily maximum and minimum variables, derived from the 6-h data simulations. Following the processing of our previous work, observational values from every station were compared directly with the nearest model points. Height differences between model topography and stations were observed because of the complexity of the topography and coastlines. Thus, before the statistical analysis, a constant lapse-rate elevation correction of 6 °C/km was applied (Barstad et al. 2009; Heikkilä et al. 2011) to both minimum and maximum temperatures. WRFEC model results were also examined and presented by grid point—station to spatially evaluate the WRF model simulation skills in detail, rather than dividing them into different sub-regions. Hence, standard statistical errors are computed, for the monthly, seasonal and annual scales, against the correspondent observational datasets.

The following standard errors statistics estimated in this study are described in Table 1[2]:

The model error was calculated as the difference between the modeled and observed values. The total error was then found by pooling together all the points of meteorological stations and not by averaging. Further analysis of the meteorological variables, regarding the representation of the extremes, was performed on daily basis, in terms of probability density function (PDF).

Additionally, a two-sided student test was performed to identify the areas with no significant differences between observed and model data at the 95% confidence level. Correlation test was also performed to examine the linear dependence between observed and model data.

2.5 ETCCDI climate indicators

To analyze spatially the climate change signal of extreme temperature and precipitation over Greece we have also calculated the extreme temperature and precipitation indices established by the Expert Team (ET) on Climate Change Detection and Indices (ETCCDI, https://www.wcrp-climate.org/etccdi). Extreme climate indices unified by ETCCDI effectively promote detection and research of extreme weather and climate change, allowing for comparison between extreme weather and climate change in different regions. The description of the extreme temperature and precipitation indices in this study is provided in Table 2.

[2] (where *"o"* is the value of the observational data, *"f"* is the simulated data).

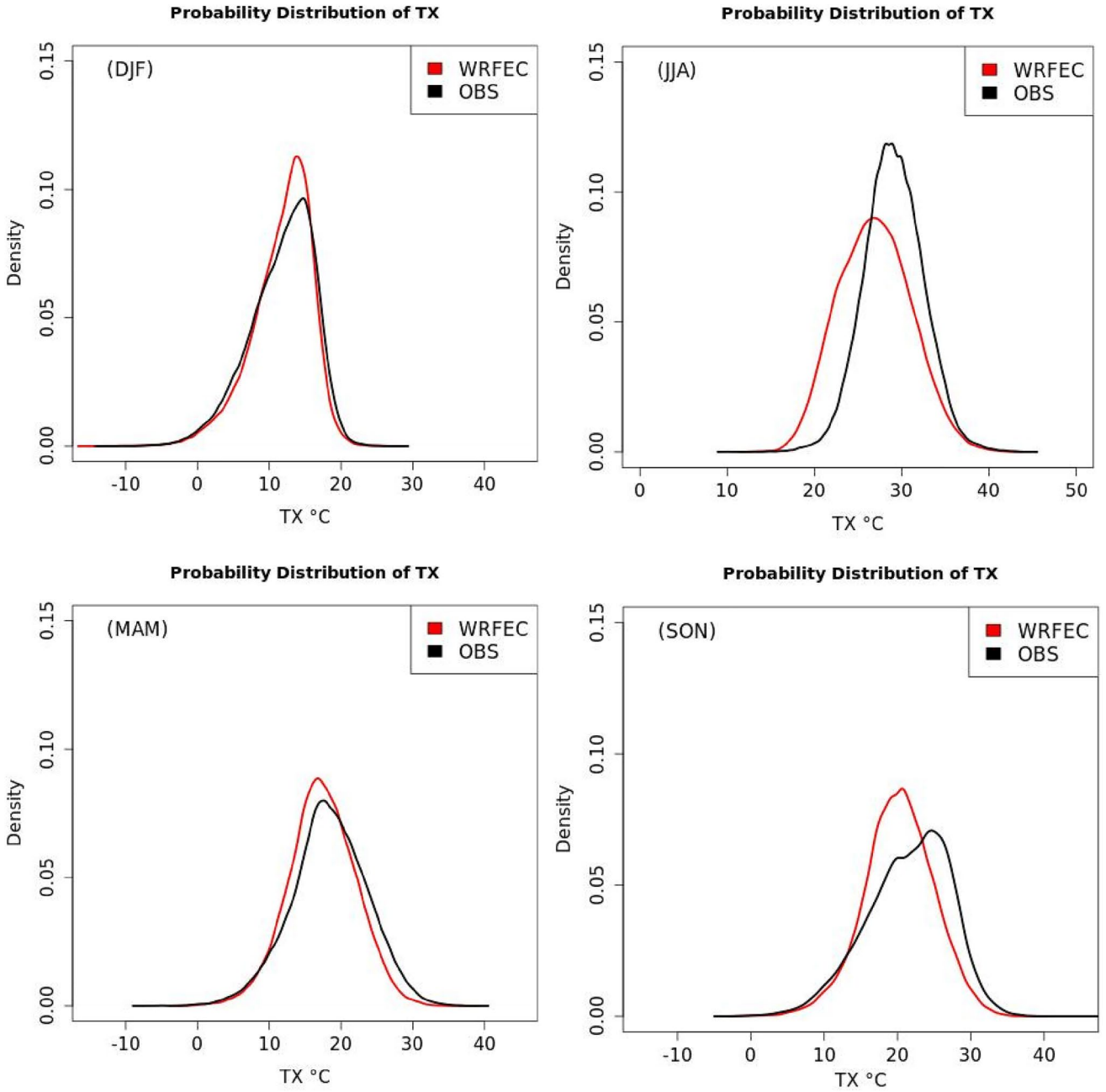

Fig. 5 Comparison of density distributions of daily TN between WRFEC and observations for all seasons for 1980–2004

3 Results and discussion

3.1 Model performance of the historical simulation

It is fundamental for climate change assessment to explore the ability of the regional model WRFEC historical simulation to represent present climate. In this section, we illustrate an overview of the model's ability to represent the mean TX, TN and RR, along with a thorough statistical analysis of the downscaled model results compared to station data.

3.2 Maximum and minimum temperatures

We firstly present the differences of mean annual variables between WRFEC Control Run (1980–2004) and station observations (OBS). The individual grid point biases between the local observational stations and WRFEC simulation are shown in Fig. S1(a.) for TX and Fig. S1(b.) for TN. It is obvious, that the biases are not consistently negative or positive regarding the temperatures. WRFEC results revealed that no pattern was observed regarding the annual

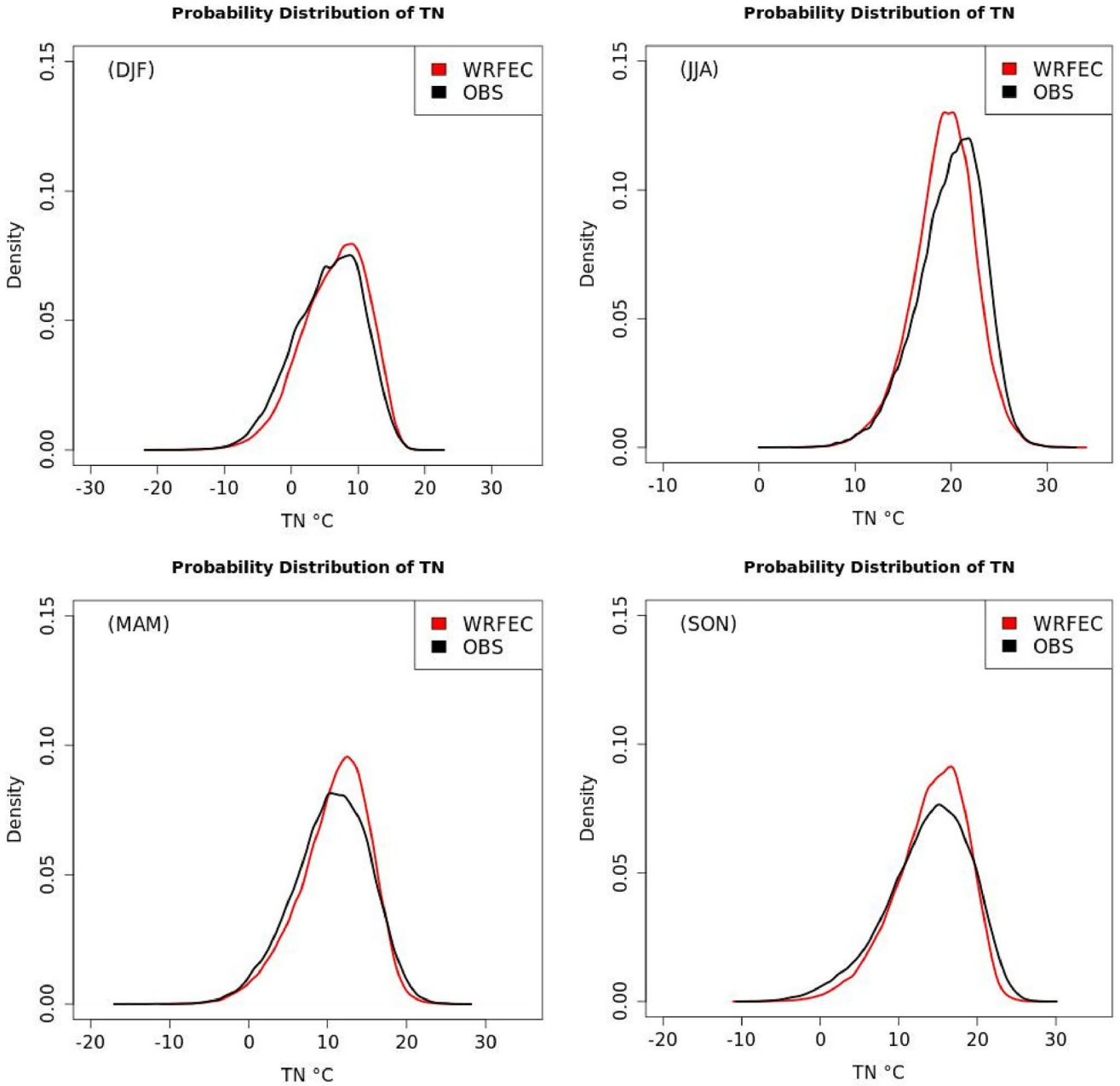

Fig. 6 Comparison of density distributions of daily TX between WRFEC and observations for all seasons for 1980–2004

minimum and maximum temperature differences between model and individual station data. It was also noticed that most of the stations had differences in the range of − 1.5 to 1.5 °C for both temperatures. WRFEC model seems to underestimate the maximum temperatures and overestimate the minimum temperatures in the majority of the available stations. It is observed that the differences of mean annual variables between modelled and observed variables of TX and TN are not enough relevant. Therefore, we also investigated the monthly and seasonal model bias. In Fig. 3a, b, the calculated mean maximum and mean minimum temperature monthly cycles, respectively, are depicted averaged over the historical period 1980–2004, along with the corresponding values of the standard deviation. The monthly mean values were calculated, for each dataset at the grid-point location of each station and then averaged over the total number of points (stations). The monthly model results of TX show an excellent agreement in the period from November to April, followed by an underestimation of the model from May to October (Fig. 3a). On the contrary, the monthly simulated TN values agree better with observations in the period from May to October (except of June) with a slight overestimation

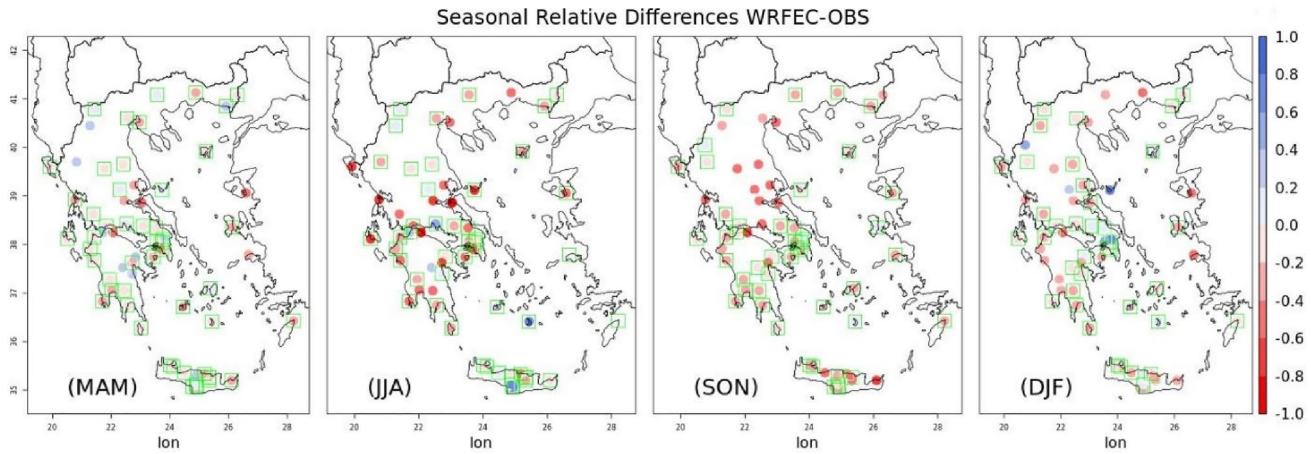

Fig. 7 Mean mean seasonal total precipitation between WRFEC Control Run (1980–2004) and station observations, (green square points specify no statistical differences between the mean distributions of seasonal RR according to Student's t test at the 95% confidence level)

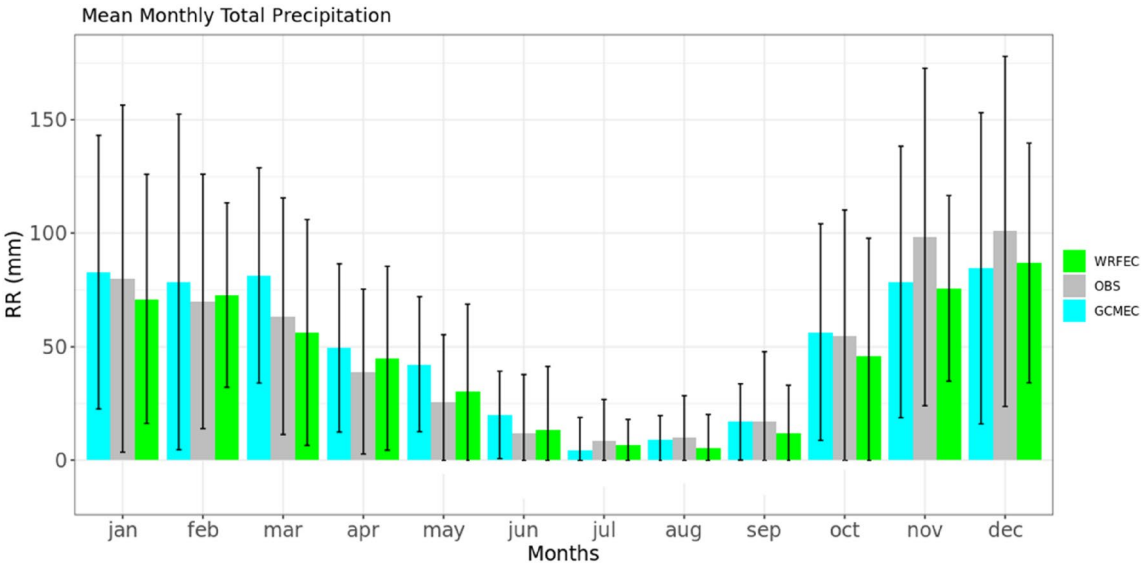

Fig. 8 Mean annual cycle of precipitation (mm/month) averaged over the historical period of 1980–2000 for the total number of stations for GCMEC, WRFEC and OSB

of the model from November to May (Fig. 3b). Overall, the monthly cycle patterns of TX and TN were well represented with WRFEC and highly correlated to the climatology of the country. The WRFEC simulation has very similar biases to the ones encountered in Politi et al. (2021), where the same model setup was forced by ERA-Interim. The higher biases are mostly associated with the warmer period months where WRFEC tends to produce lower maximum temperatures, while higher minimum temperatures are found during the colder months. The results indicate that GCMEC reproduces the observed monthly TX cycle but underestimates it. The performance of the global model improves in the case of monthly TN values, but it does not outperform the WRFEC model.

Figure 4 depicts the differences of 25 years seasonal mean maximum temperature and minimum temperature compared to the stations, respectively. The seasonal means are shown for winter (December, January, and February, DJF), spring (March, April, and May, MAM), summer (June, July, and August, JJA), and autumn (September, October, and November, SON). Smaller seasonal differences of maximum temperature are observed during the winter period in the range of − 1 to 1.5 °C. In particular, during winter there is a north–south gradient towards negative differences. On the other hand, the highest differences (above − 5 °C) are

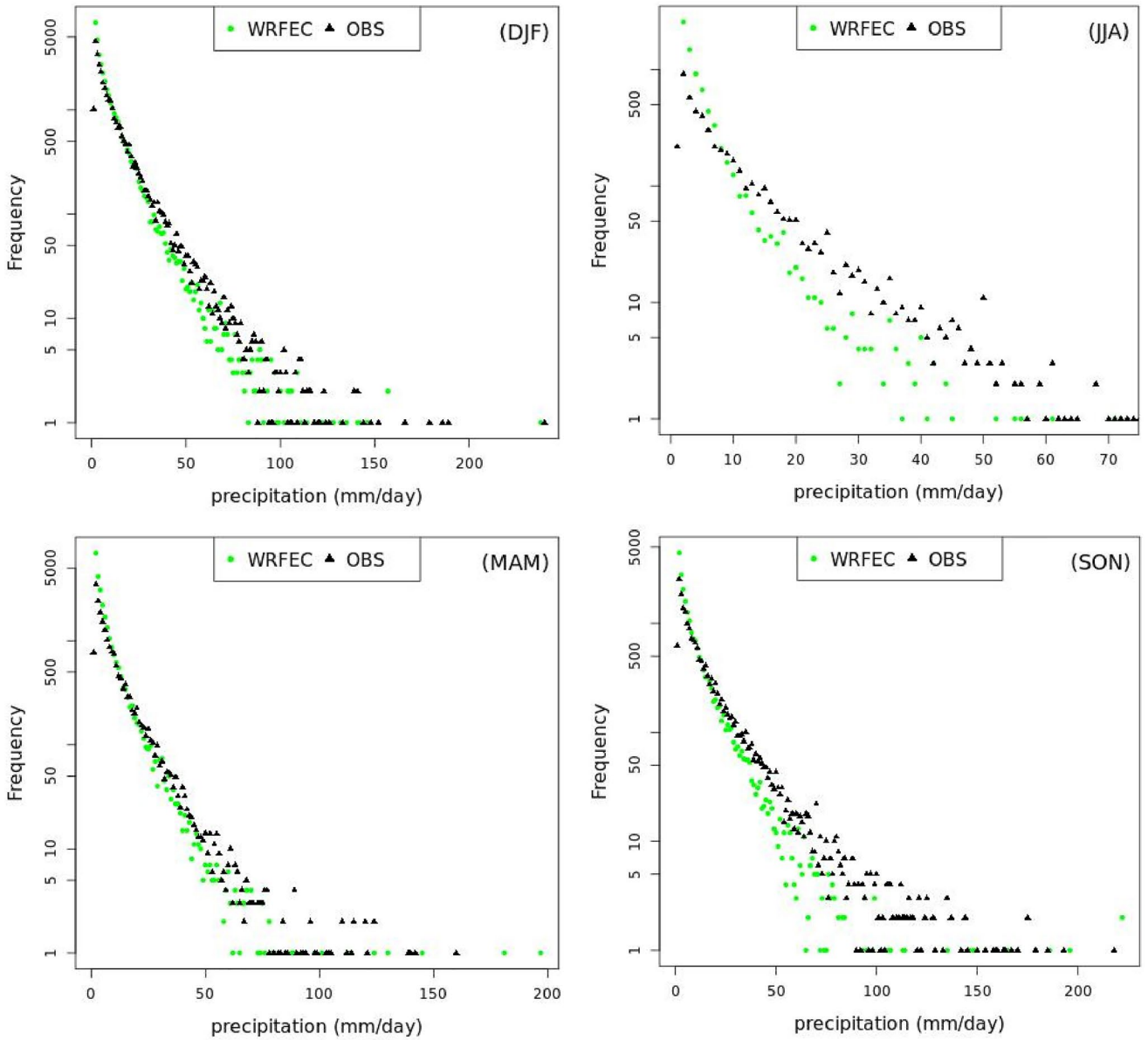

Fig. 9 Comparison of frequency distributions of daily precipitation between WRFEC and observations for all seasons in the period 1980–2000

obtained during summer in a few coastal stations. Furthermore, the results showed more station locations with positive differences during spring and winter season, while negative differences are seen mainly during autumn, for the seasonal TX.

Regarding the minimum temperatures, positive differences are found mainly during spring. The greater differences of about − 2.5 to 2.5 °C, are noticed during the summer period. Positive differences higher than 2 °C (> 2 °C) are also calculated in winter. It is observed that the majority of the stations with no statistically significant differences (green square points) in the mean values (− 0.5 to 0.5 °C) for TX, is observed during spring and winter seasons, while for TN during autumn and winter. The model presented also greater negative seasonal differences during summer regarding the minimum temperature in most areas, something that underlines the trend of the model to reduce minimum temperature in summer.

To assess our downscaled global model quantitatively, we proceeded to the statistical evaluation of the simulated mean fields from WRFEC with historical observations of the examined variables. The statistical errors (as described in Sect. 2.4) show the ability to represent the mean structure of the surface variables at different temporal scales for monthly to annual averages. The statistical analysis results of TX and TN were calculated using available observational data

a

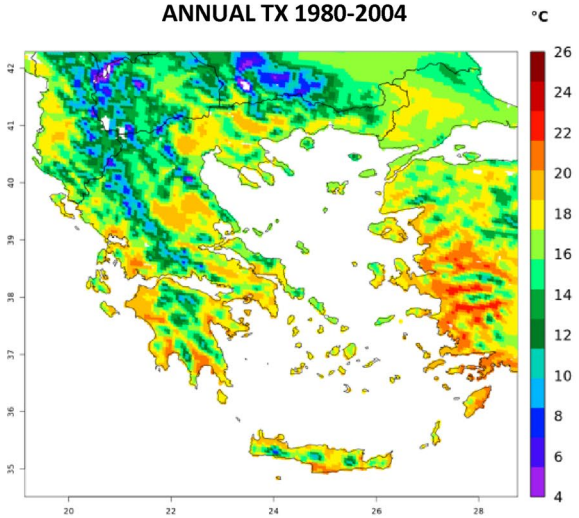
ANNUAL TX 1980-2004
°C
26
24
22
20
18
16
14
12
10
8
6
4

b

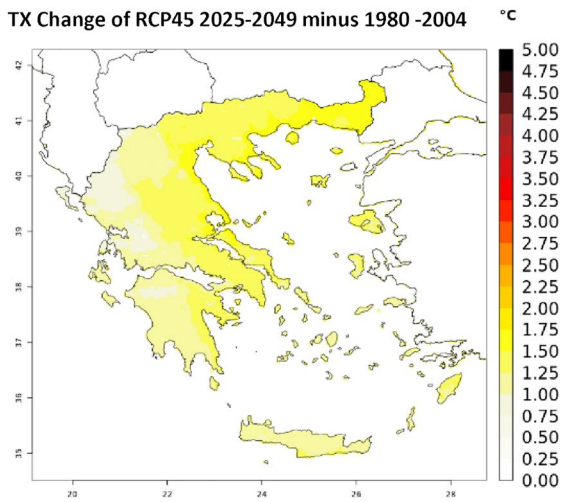
TX Change of RCP45 2025-2049 minus 1980 -2004
°C
5.00
4.75
4.50
4.25
4.00
3.75
3.50
3.25
3.00
2.75
2.50
2.25
2.00
1.75
1.50
1.25
1.00
0.75
0.50
0.25
0.00

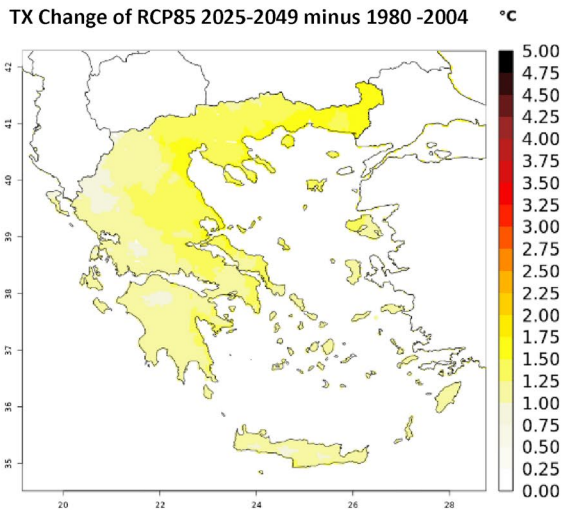
TX Change of RCP85 2025-2049 minus 1980 -2004
°C
5.00
4.75
4.50
4.25
4.00
3.75
3.50
3.25
3.00
2.75
2.50
2.25
2.00
1.75
1.50
1.25
1.00
0.75
0.50
0.25
0.00

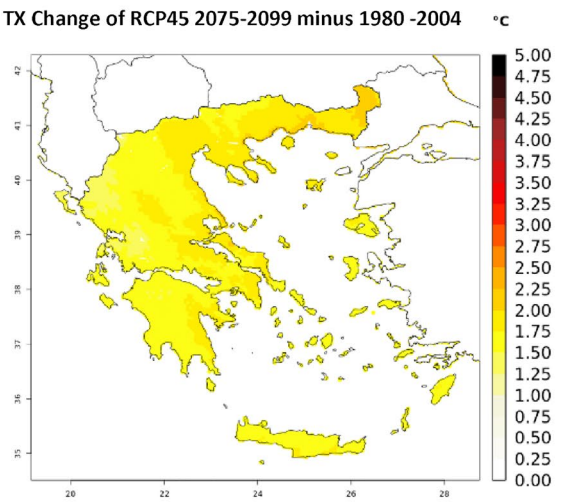
TX Change of RCP45 2075-2099 minus 1980 -2004
°C
5.00
4.75
4.50
4.25
4.00
3.75
3.50
3.25
3.00
2.75
2.50
2.25
2.00
1.75
1.50
1.25
1.00
0.75
0.50
0.25
0.00

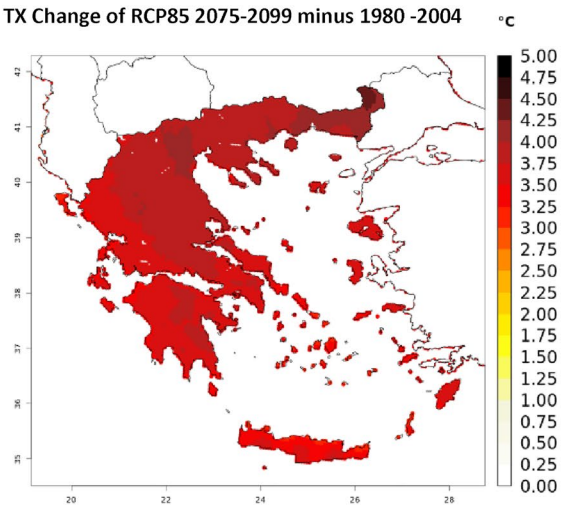
TX Change of RCP85 2075-2099 minus 1980 -2004
°C
5.00
4.75
4.50
4.25
4.00
3.75
3.50
3.25
3.00
2.75
2.50
2.25
2.00
1.75
1.50
1.25
1.00
0.75
0.50
0.25
0.00

◂**Fig. 10** **a**. WRFEC annual mean historical climatology, **b**. WRFEC climate change differences for daily maximum temperature (2025–2049 minus 1980–2004 and 2075–2099 minus 1980–2004) for RCP4.5 and RCP8.5. (Areas with no dots specify statistically significant changes using a Student's t-test at the 95% confidence level)

from the weather stations over the entire domain (Table 3). The approach for analysis also involved the investigation of the driver data performance of the global model EC-EARTH (GCMEC) by comparison with the observational data and WRF-EC output to showcase the added value of the downscaling methodology. Bias results of WRF-EC for all temperatures and time scales presented consistent values, which did not vary significantly between them, with cold bias around 1.1 °C for maximum temperature and a warm bias of 0.24 °C for minimum temperature. The monthly, seasonal and annual scales correlation coefficients for TX and TN varied, of which seasonal values yielded the highest correlation of 0.95 and 0.94, respectively. In general, RMSE and MAE statistics progressively reduced along time scales, with the lower errors being identified on the annual scale. The efficiency scores of MIA and NSE showed an improved performance of the model on the seasonal scale with a range of values of 0.83–0.88. Furthermore, the statistical errors of WRF-EC presented improved values against GCMEC. Both temperatures of GCMEC revealed a colder bias (− 2.98 °C for TX and − 0.4 °C for TN). It is worth to mention here, that WRF-EC produced an improved bias of TN, not only compared to GCMEC but also to the one of the downscaled reanalysis datasets with WRF in the study of Politi et al. (2021). In addition, the RMSE and MAE metrics of the global model were larger than the ones of WRF-EC. Moreover, the efficiency metrics showed an improved performance of WRF-EC compared to the driver global model for all temporal scales. Thus, the statistical analysis of temperatures reveals a very good performance of the WRF-EC model and highlights the added value of the downscaled fields compared to those of the forcing GCM.

Additionally, a worthwhile downscaling methodology should have the ability to simulate climate extremes well. For this reason, we assess the quality of our downscaled results based on the realistic simulations of extremes of daily TX, TN, and RR for each season. Figure 5 shows the seasonal probability distributions of the daily minimum temperature for WRFEC model and station data.

The median TN was underestimated by the model during the summer period, showing a significant shift towards colder values. Overall, the WRFEC simulations were in good agreement with the observations along with the distribution tails, during all seasons, with a very slight shift of the median TN towards warmer values, in winter, spring and autumn. Regarding the probability distribution of maximum temperature, illustrated in Fig. 6, there was a significant shift towards lower temperature values in summer with lower density values. The median TX was also underestimated by the model during autumn but with higher density values than the observational data. A slightly maximum temperature underestimation by the model compared to observations was observed for winter and spring. From the comparison of temperature percentiles for extreme values of model results versus observations (Fig. S2), a very good agreement is found in 90th, 95th and 99th percentiles of TN while a slight overestimation is obtained with the model in the coldest TN values (5th and 10th percentiles). The highest percentiles of TX (higher than 90) are slightly underestimated by the model. The two-sided Kolmogorov–Smirnov (KS) test was applied on daily data for each season and returned estimations of p-values < 0.05 which rejected the null hypothesis of equal distribution between models and observations. In addition, the calculated the Kolmogorov–Smirnov distances between simulated (WRFEC and CGMEC) and observed data provided a quantitative assessment of the added value of downscaling results. The comparison indicated that the high-resolution WRFEC model returned lower values of (KS) D than those of GCMEC on average for both temperatures and all seasons.

In what concerns the statistical results, Cardoso et al. (2019) reported that in the case of Portugal, EUROCORDEX models showed a cold bias regarding the maximum temperature and declared that those biases were clearly inherited from the forcing GCM since different RCM forced by the same GCM produced similar bias; on the other hand, the internal model variability played a stronger role in minimum temperature. Similarly, to the previously mentioned study, our findings of a cold GCM bias in TX is inherited also by WRF (Table 3). On the other hand, the sign of the TN bias changes in between the coarse (GCMEC) and downscaled simulations (WRFEC).

The slight poor performance of WRFEC for summer temperatures (a strong underestimation in summer TX and TN) could be probably related to boundary conditions deficiencies inherited by the GCM and/or due to the internal model dynamics and physics (Giorgi et al. 2001; Dasari et al. 2014). Further investigation is about to be conducted but it's beyond the scope of this paper.

3.3 Precipitation

Model results were overall in agreement with the climatology of Greece, where the precipitation patterns were generally higher during the late autumn and winter months, along with the most significant amounts of rainfall. The results also yielded higher precipitation amounts over mountainous areas and in the western parts of the country that were strongly associated with the orography, and the fact that almost all low-pressure systems crossing the country and resulting in

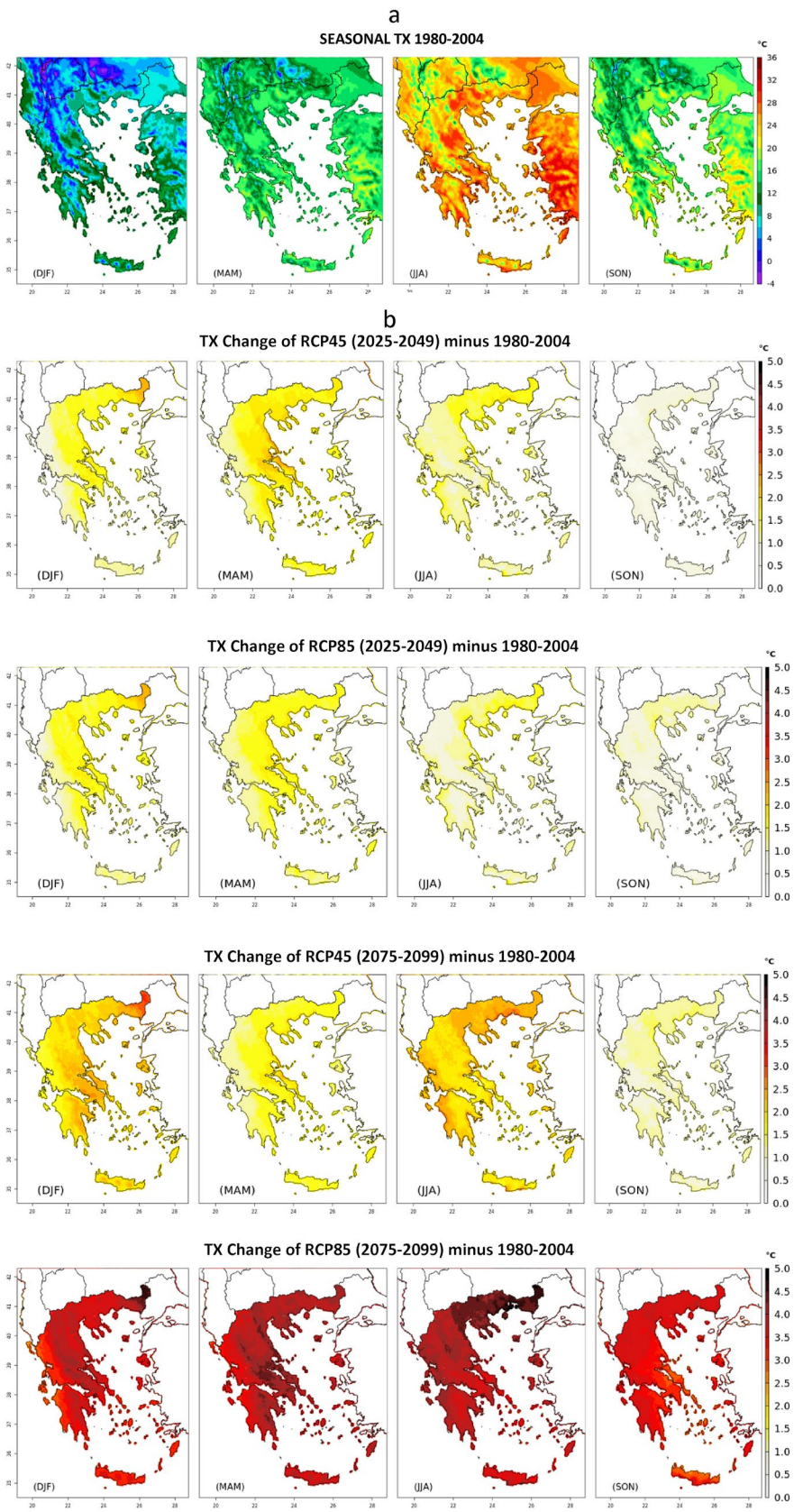

Fig. 11 **a** WRFEC mean historical climatology, **b** WRFEC seasonal climate change signal for daily maximum temperature (2025–2049 minus 1980–2004 and 2075–2099 minus 1980–2004) for RCP4.5 and RCP8.5. (Areas with no dots specify statistically significant changes using a Student's t-test at the 95% confidence level)

intense rainfall come from the west. Indeed, during fall and winter prevailing westerly winds from the Ionian Sea hit the west coasts and the mountain range of central mainland (Pindos), generating precipitation all along the west region of Greece. Thus, the orographic precipitation is an important phenomenon that affects a large portion of the west part of the country. The windward side of a mountain affected by prevailing winds is usually wetter and the leeward side of the mountain is usually dryer due to the moisture released when precipitation occurs. WRCEC results are in line with the climate atlas that has been developed by HNMS) (available at http://climatlas.hnms.gr/sdi/?lang=EN), also described in detail in the hindcast analysis by Politi et al. (2021). In the study area, the good representation of the major mountainous locations and coastline obtained with the downscaling approach allows the production of cyclogenesis and the associated orographic wind systems whatever the quality of the large scale circulation provided at the RCM's boundaries by the global model (Politi et al. 2021) (Fig. 7).

The annual relative differences (in fraction) in Fig S3 showed a consistent pattern of underestimated annual precipitation from WRFEC in the range of 0.2 to 0.4, in the west and north stations of the country. The seasonal relative differences illustrated in Fig. 8b, revealed that WRFEC overall reproduced well the observations, with a general small dry bias (up to − 0.4) during all seasons and a few localized exceptions of wet bias, in accordance with the results described by Soares et al. (2017). More specifically, it was found that particularly in summer and less in autumn, WRFEC underestimated slightly the precipitation in parts of the west and central Greece. On the annual temporal scale, almost half number of the stations (29 out of 66) do not present statistically significant differences in the mean values between the observed and simulated points (Fig. S3). On the seasonal scale, the majority of the station points have no statistically significant differences among observed and model mean values during all seasons (Fig. 7). On average, only around 10 stations out of 66 present statistically significant differences with the higher number of stations found in autumn and winter seasons. In addition, the model showed some difficulty in describing some regions characterized by high relative differences, probably due to coarse station density which is associated with the complex topographical features. The light seasonal rainfall under-prediction was over most parts of the country, but with good description of the spatial precipitation pattern.

The WRFEC mean annual cycle of monthly total precipitation (Fig. 8) was sufficiently represented by the model concerning the maximum values in the winter and minimum ones in the summer. In comparison with observations, WRFEC generally underestimated the rainfall amounts. The under-prediction was observed in January and between March and April, while from April to June the model slightly overestimated precipitation. In particular, the model's performance in June and July was strikingly accurate, however from August to December the performance of the model reversed, resulting in lower precipitation values than the observations, particularly in November and December. Yet, it should be emphasized that the rather large error bars in all datasets analyzed are due to the large spatial variability of precipitation in the study area (Hatzianastassiou et al. 2008). Overall, GCMEC tends to overestimate the values from January to July, and indicates a better performance compared to WRFEC only in January, August, September and October.

Regarding the precipitation statistical errors over the entire domain (Table 3), the values of COR, NSE, and MIA remained lower than those on temperatures. In general, the WRFEC model underestimated precipitation compared to observations on monthly and seasonal scales (less than 10%) but presented a very good performance on the annual scale with a small positive pbias of 2.9%. On the other hand, GCMEC consistently overestimated precipitation (around 14% in all temporal scales). As in the case of temperatures, the seasonal values of WRFEC precipitation yielded the highest correlation of 0.57, larger than that of the GCMEC value (0.45). In general, the WRFEC model yielded a noticeable improvement on precipitation compared to GCMEC according to the error statistics (Table 3). Also, those statistics presented a very much improved agreement when compared to the study of Kotlarski et al. (2014) that reported precipitation biases in the ± 40% range, regarding the EUROCORDEX ability to represent the European precipitation.

The seasonal frequency distribution of daily precipitation (Fig. 9) was plotted on a logarithmic scale with bins of 1 mm to highlight the extremely strong precipitation rates.

Overall, the model underestimated the precipitation events below 100 mm/day in winter and autumn but could produce more extreme events during those periods. Noticeable is the case where the model produced in excess precipitation events (above 150 mm/day) compared to observations during spring. That might be caused either by the model or by the station density that could be too low to accurately satisfy the WRFEC resolution, particularly over mountainous areas.

Furthermore, for the longer-term temporal statistics (e.g., seasonal, annual), which are of interest to the present study, the added value in higher-resolution simulations is not always evident in current RCMs. Downscaling with a limited area model as WRF contributes to partly replicate the inaccurate feature of the large scale field from the global model even in the boundary layer where small scale processes dominate its dynamics. For example, comparisons between

a

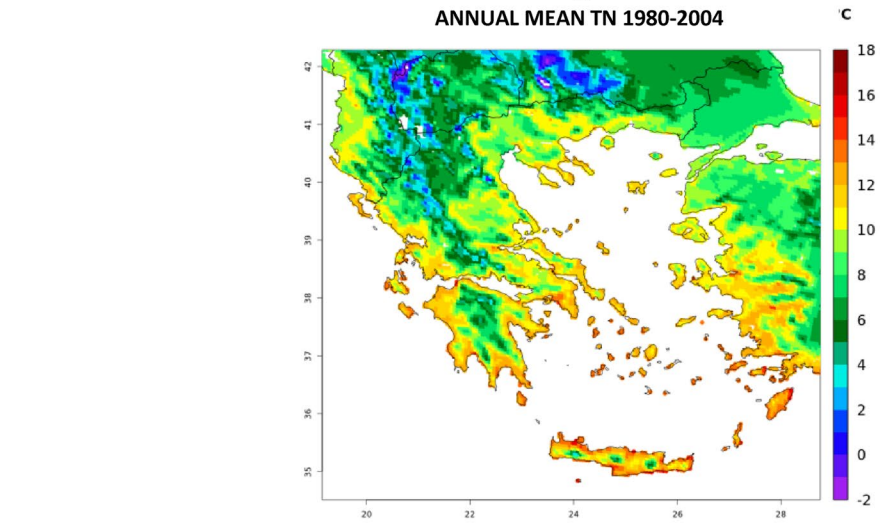
ANNUAL MEAN TN 1980-2004
°C
18
16
14
12
10
8
6
4
2
0
-2

b

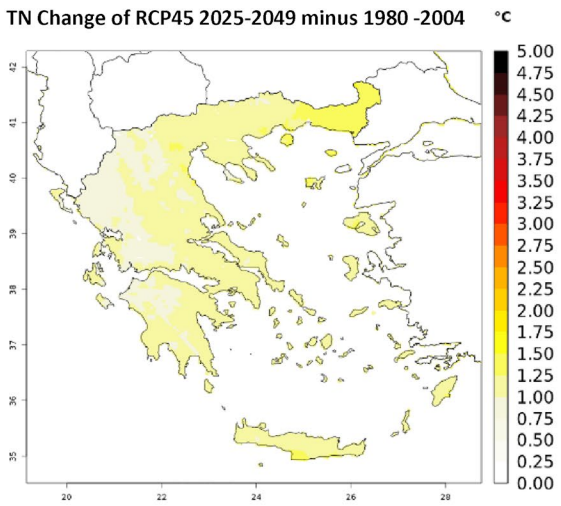
TN Change of RCP45 2025-2049 minus 1980 -2004
°C
5.00
4.75
4.50
4.25
4.00
3.75
3.50
3.25
3.00
2.75
2.50
2.25
2.00
1.75
1.50
1.25
1.00
0.75
0.50
0.25
0.00

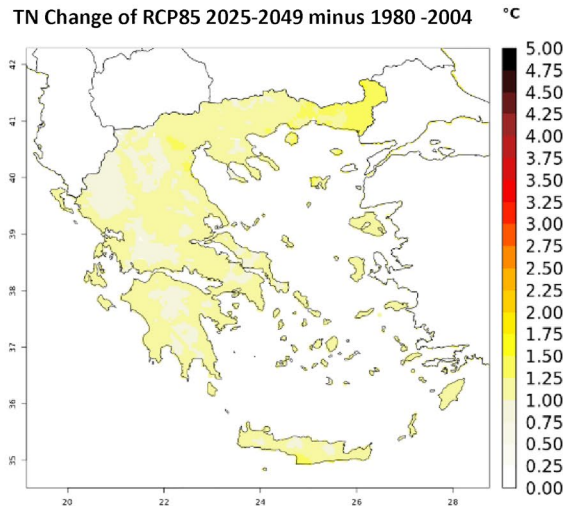
TN Change of RCP85 2025-2049 minus 1980 -2004
°C
5.00
4.75
4.50
4.25
4.00
3.75
3.50
3.25
3.00
2.75
2.50
2.25
2.00
1.75
1.50
1.25
1.00
0.75
0.50
0.25
0.00

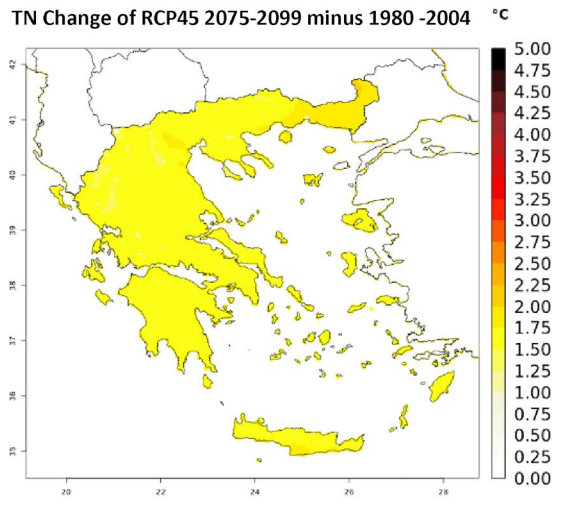
TN Change of RCP45 2075-2099 minus 1980 -2004
°C
5.00
4.75
4.50
4.25
4.00
3.75
3.50
3.25
3.00
2.75
2.50
2.25
2.00
1.75
1.50
1.25
1.00
0.75
0.50
0.25
0.00

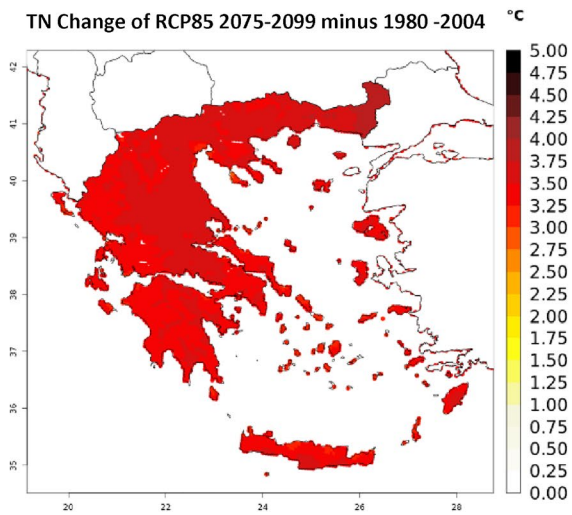
TN Change of RCP85 2075-2099 minus 1980 -2004
°C
5.00
4.75
4.50
4.25
4.00
3.75
3.50
3.25
3.00
2.75
2.50
2.25
2.00
1.75
1.50
1.25
1.00
0.75
0.50
0.25
0.00

◂**Fig. 12** **a**. WRFEC annual mean historical climatology, **b**. WRFEC climate change signal for daily minimum temperature (2025–2049 minus 1980–2004 and 2075–2099 minus 1980–2004) for RCP4.5 and RCP8.5. (Areas with no dots specify statistically significant changes using a Student's t-test at the 95% confidence level)

0.11° and 0.44° EUROCORDEX experiments indicated no systematic temperature bias reduction in the high-resolution experiments, while for precipitation, seasonal mean biases could be larger in the higher-resolution EUR-11 set of simulations (Kotlarski et al. 2014; Soares and Cardoso 2018; Zittis et al. 2019). Although our simulation has some biases in most variables, no significant departures are noticeable from observations. It is also a positive outcome that the model brings high detail in the spatial patterns and added value to the probability distributions, as the simulated frequency distribution of the precipitation and temperature extremes from the 5-km WRFEC is consistent with the observed structure and extreme values.

4 Future projections

4.1 Future projection of minimum and maximum temperatures

WRFEC represented very well the geographical distribution of annual and seasonal mean daily TX and TN (Figs. 10a, 11, 12, 13a) in the historical period and clearly illustrated the seasonal variation with similar ranges of temperature values also found in the previous study of Politi et al. (2021).

The annual mean and seasonal projected changes along with the spatial distribution of the historical period are depicted in Figs. 10, 11, 12 and 13. In general, the warming projections for the far future show larger changes for maximum than for minimum temperature, for both scenarios, and for the annual mean and seasonal temperatures. On the other hand, the projected changes are less intense during the near future with GCM differences under the two scenarios. According to a 2-tailed t-test, the projected changes seen in all figures are statistically significant at the 95% confidence level over the entire region. It is obvious from these figures that the mean temperatures derived from maximum and minimum temperatures increase consistently, but with different magnitudes across the regions and emission scenarios.

Because of the higher greenhouse gas emissions and radiative forcing of RCP8.5 by the end of the century, the magnitude of the mean annual maximum temperature warming for RCP8.5 is greater than that for RCP4.5 (Fig. 10). According to the RCP4.5, the largest warming is obtained over the eastern part of the country (some northeastern inland parts and eastern coasts) reaching up to 2 °C in the period 2025–2049 and extends more towards southeastern areas up to 2.5 °C in the period 2075–2099. In the case of the RCP8.5 scenario, the difference between the two future periods is remarkably more pronounced and the mean daily TX is found to increase up to 4.5 °C in the far future, particularly in some eastern and coastal parts. It is also observed that the pattern of changes is clearly linked to the orography of central Greece and the island of Crete.

The investigation of the projected changes for the seasonal maximum temperature revealed a relative seasonality (Fig. 11). There is a different spatial pattern of temperature (TX) change for each season. Under both RCPs, there are significant regional differences in terms of projected temperature increase in each season. Under the RCP8.5 in the far future period, WRFEC projects a robust magnitude of warming over the whole country. The model predicts maximum TX increases in the range of 2.75 and 3.75 °C in winter and autumn, but in summer and spring the changes reach values from 3 °C, near the coast, up to 5 °C in some inland areas and in the north-eastern Greece. In the near future, TX increases mark a west–east gradient in spring and winter in the range of 0.75 to 2.5 °C, which is profoundly linked to the orography of central mainland. The lower projected changes are observed in winter with TX increases from 0.75 to 1.5 °C under both RCPs and only in the near future period.

Considering the mean daily minimum temperature in RCP4.5, increases are projected up to 1.5 °C in northeastern regions in the near future and, in the range between 1.75 and 2.5 °C in the far future (Fig. 12). RCP8.5 shows a much greater warming than RCP4.5 by the end of the century with a west–east gradient, reaching values from 3 up to 4 °C. TN is expected to increase up to 3.5 °C near the coasts and the islands of the central Aegean Sea, while the increase will be a little higher in the islands of the north and eastern Aegean area. Overall, the projected changes for the minimum temperature in the far future, according to both scenarios, are similar to the changes of the maximum temperature, but with mitigated properties; the changes are less sharp with smaller contrasts and the west–east gradient also less intense.

Under RCP4.5, the magnitude of the warming in autumn is the lowest of all seasons with values around 0.5–1 °C (Fig. 13). During the summer and winter seasons of the future period 2075–2099, the WRF simulation projects a higher temperature increase of 2–2.5 °C in the entire country, uniformly. During winter in the near future projection, the largest warming occurs over some inland parts and northeastern Greece. The model projects a small west–east gradient of warming in spring, for both future periods. Under RCP8.5 and during the near future projection, the model produced much milder warming (especially during autumn) in the range of 0.75–2.5 °C with the higher temperature increase in the northeastern part of the country and some coastal areas. However, during the far future period, the model's projection in summer

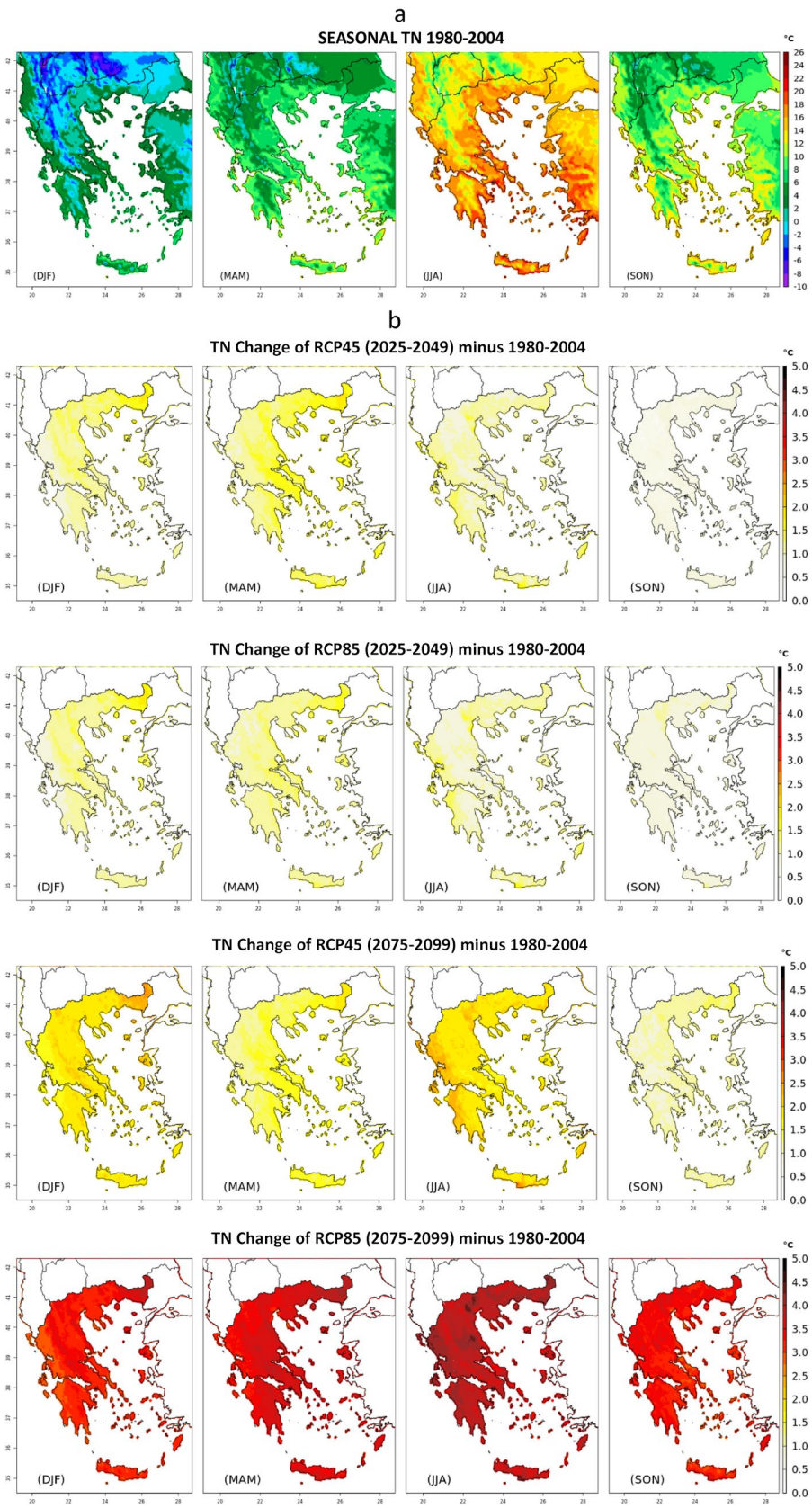

Fig. 13 **a** WRFEC mean historical climatology, **b** WRFEC seasonal climate change signal for daily minimum temperature (2025–2049 minus 1980–2004 and 2075–2099 minus 1980–2004) for RCP4.5 and RCP8.5. (Areas with no dots specify statistically significant changes using a Student's t-test at the 95% confidence level)

predicts larger magnitude of warming over the western part of mainland, the Ionian Islands and, in some plain parts of central and northern mainland and southern Crete. In these areas, the highest maximum temperatures are usually observed during summers. According to the projections, the high increases will impact these areas adversely. During winter, the model projects notably the most significant warming over the mountainous areas, while in spring, the temperature increases are smaller in the western than in eastern parts of the country.

In similar previous studies, based on global and regional models, projected changes were found to be rather uniform, as relatively small-scale climate features and feedbacks were smoothed due to the coarser resolution. In general, Wagner et al. (2013) explained that the projected climate change signals of the coarse domain were transferred to the fine resolution without strengthening or weakening the climate change signal; but the higher resolution added some more detail in the spatial patterns as expected.

In what concerns temperature change signal, WRFEC simulation projects an annual mean warming over Greece, which is significant at the 95% confidence interval for all grid points. In general, during the far future period, the model projects a robust magnitude of warming with most pronounced changes over the whole country under the RCP8.5 scenario. This conclusion is in accordance with Varotsos et al. (2021a) who examined the impacts of climate change on the tourism sector from a large ensemble member of RCMs from the EUROCORDEX under three RCP emissions scenarios. Overall, the warming projections for far future show larger changes for maximum than for minimum temperature, under both scenarios, and for the annual mean and seasonal temperatures. On the other hand, the projected changes are less intense during the near future with no significant differences under the two scenarios. The model predicts TX increases in the range of 2.75 and 3.75 °C in winter and autumn, but in summer and spring the changes may range from 3 °C, near the coast, up to 5 °C in some inland areas and in north-eastern Greece. In the near future, TX increases mark a west–east gradient in spring and winter in the range of 0.75 to 2.5 °C, which is profoundly linked to the orography of central Greece. The results are generally consistent with previous studies indicating that the Mediterranean region and southern Europe will exhibit an amplified temperature increase in comparison to the rest of the continent (Giorgi et al. 2004). Our findings are also in agreement with the most recent study of Coppola et al. (2021) that estimated for RCP8.5 during summer late century period maximum signal over the Mediterranean land regions (where Greece is included) of around 4.5 °C with EUROCORDEX ensemble and 6.5 °C with CMIP6. The lower projected changes are observed in the winter with TX increases from 0.75 to 1.5 °C under RCP4.5 and RCP8.5 and only in the near future period. Overall, the projected changes for TN in far future, according to both scenarios, are similar to the changes of TX, but less sharp with smaller contrasts and the west–east gradient also less intense.

4.2 Future projection of precipitation

The signal of climate change on the annual precipitation over Greece given by the WRF simulation is shown in Fig. 14b. All the results point out to a general decrease of the annual precipitation all over the eastern part of the country (with islands included). However, an increase of 20% is projected in the western areas only in the near future and without statistical significance. Although in the less severe scenario (RCP4.5) the decreases of rainfall are smaller than RCP8.5, there is a significant reduction in the range of − 30 to − 40% in areas like the island of Evia and in small areas of the central mainland. This reduction, according to the RCP8.5, becomes more extended towards the western parts of the country, particularly in the far future. More specifically, the model indicates decreases around − 25% throughout most parts of the domain. Additionally, the most dramatic reductions above − 30% and in some cases up to − 50% are found in eastern Crete, eastern Peloponnese, central mainland and in few areas of the eastern part of the country.

The projections for the seasonal precipitation changes under RCP4.5 and RCP8.5 are depicted in Fig. 15. Under RCP4.5, the precipitation reduction is projected to values over 30% in eastern Greece. The model also estimated statistically non-significant changes of increasing rainfall during autumn around 10% in some small areas all over the country and, only in western Greece during all the other seasons of both future periods. The most dramatic reductions (above 40%) of seasonal precipitation are observed under RCP8.5 in the far future covering almost all the country. In all seasons, small positive and negative changes are projected of around 10%, located mostly in the western parts of the mainland, the Ionian Islands and western Crete. Nevertheless, these changes are non-significant in most areas of the country. In general, the total annual projected changes are related to the reduction of precipitation during winter, spring and autumn, since the summer precipitation contributes the minimum to the annual total.

PDF distributions of daily precipitation intensity in the present and future climate scenarios are depicted in Fig. 16 below. All distributions are similar to each other up to the precipitation bin of around 60 mm, where the transition between reduction and increase of frequency of extreme precipitation occurs. This rainfall amount corresponds to the 99th percentile in historical and future climate periods. An increase of extreme rainfall amount (above ~ 300 mm/

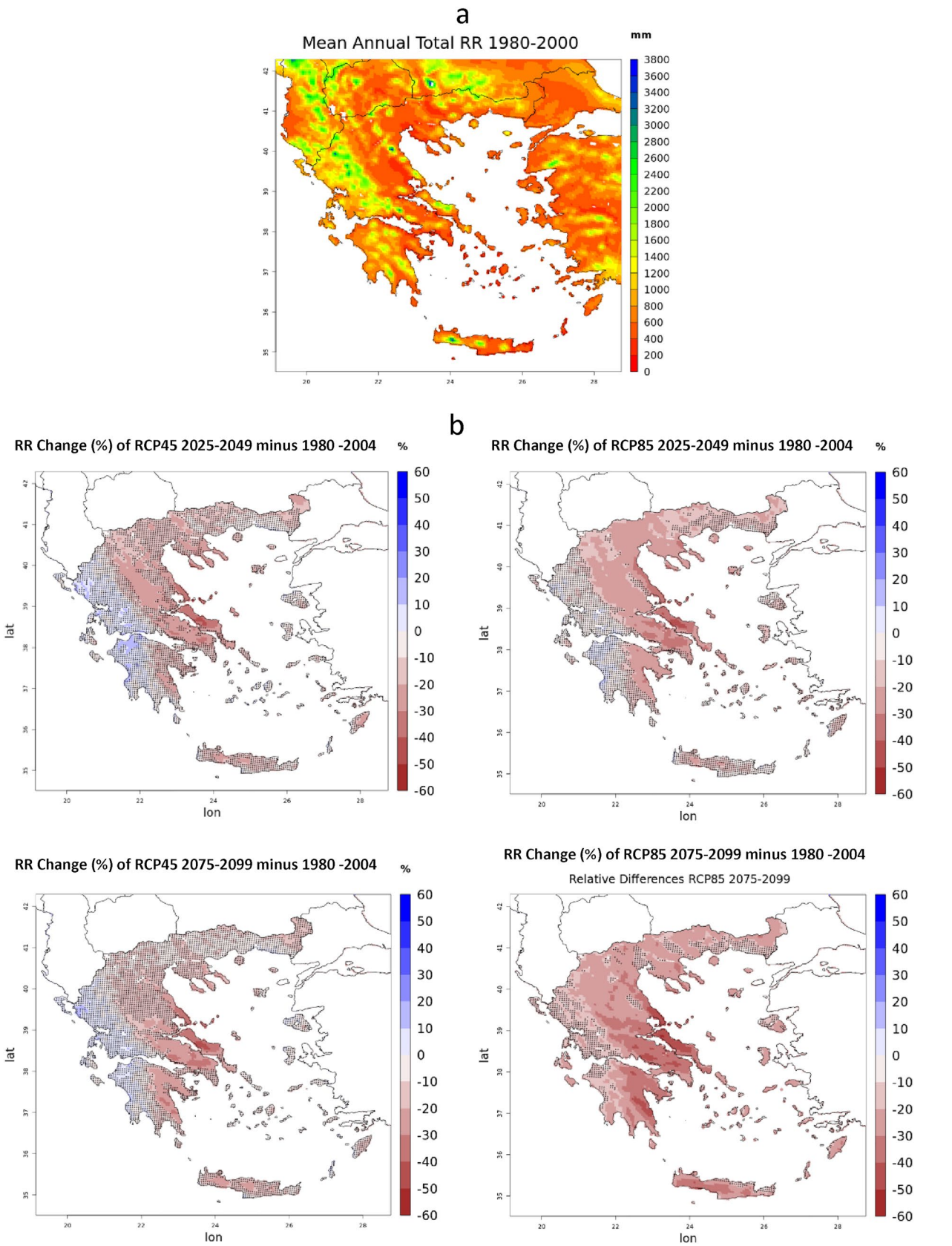
a
Mean Annual Total RR 1980-2000
mm
3800
3600
3400
3200
3000
2800
2600
2400
2200
2000
1800
1600
1400
1200
1000
800
600
400
200
0
b
RR Change (%) of RCP45 2025-2049 minus 1980 -2004
%
RR Change (%) of RCP85 2025-2049 minus 1980 -2004
%
RR Change (%) of RCP45 2075-2099 minus 1980 -2004
%
RR Change (%) of RCP85 2075-2099 minus 1980 -2004
Relative Differences RCP85 2075-2099
lat
lon
60
50
40
30
20
10
0
-10
-20
-30
-40
-50
-60

◂**Fig. 14** **a** WRFEC mean historical climatology, **b** annual mean precipitation relative changes given by WRFEC for RCP4.5 and RCP8.5 (2075–2099 minus 1980–2004)/1980–2004. (Areas with dots specify changes not statistically significant using a Student's t test at the 95% confidence level)

day) is obtained under the future scenarios with a rather low frequency of occurrence.

The projected changes for precipitation are in accordance with the studies of Tolika and Zanis (2012) and Maheras et al. (2008) that also reported that Greece would experience a persisting absence of rainfall. More specifically, the climate change signal of precipitation over Greece revealed a general decrease of the annual precipitation all over the eastern part of the country (with islands included) with the most dramatic reductions, above − 30% and in some cases up to − 50%, found in eastern Crete, eastern Peloponnese, central mainland and in few areas of the eastern part of the country. However, the large increase for summer precipitation in both scenarios in western Greece is most-probably related to a more south-westerly flow in the simulated historical period. Summertime precipitation during the historical period is considerably strong (see Fig. 9), probably due to the convection-permitting setup and related to these isolated and usually very local events particularly in the period 2025–2049. This internal variability of simulation was also found in the study of Knist et al. (2020). Under RCP4.5, notable summer increases in the southerly flows were estimated up to 40%, which combined with large-scale subsidence, could cause a significant rise in the occurrence of heat wave events (Karozis et al. 2021). The latter study which was part of our work revealed that estimated changes in the air mass flows under future high-emission scenarios imply changes in their associated synoptic patterns. Compared to our results, the changes in the total precipitation were found less pronounced under both the RCP4.5 and RCP8.5 in the period 2031 and 2060 over Crete in a study of Varotsos et al. (2021b) for 5 RCM's CORDEX ensembles. The differences between the two scenarios in summer were large in eastern Greece, indicating a great natural variability over the region. For example, in some areas (Crete, eastern coastal parts of central Greece), the change was a decrease in RCP4.5 but an increase in RCP8.5. Similar findings between the two scenarios were obtained in the study of Chen et al. (2019) for the projected changes in eastern Asia which is characterized by complex topography.

4.3 Projective changes of ETCCDI

In this section, we present the computed differences in climate indices between the two future and historical periods. The statistical analysis results presented in Sects. 3.1–3.2 using the GCM (EC-Earth) coarser data and the downscaled simulations against temperature and precipitation observations demonstrate the capability of WRFEC to capture the basic climate characteristics of Greece. This provides confidence on using WRFEC simulations to calculate ETCCDI climate indices. Furthermore, the comparison of GCMEC and WRFEC calculated ETCCDI indices with those calculated using observational station data is carried out to highlight the added value of using the higher resolution simulations of 5 km on the upper panel of Figs. 17, 18, 19, 20, 21, 22, and 23, for the reference period 1980–2004. The comparison with observations clearly indicates the improvement in all calculated ETCCDI indices with WRFEC against those of GCMEC at the locations of the stations.

The changes in the number of days where daily TX was above 25 °C (summer days, see Fig. 17) appeared to have an increasing frequency for both scenarios and periods with less intense increase of an average of 5–20 days during the near future period in the mountainous and inland regions and 25 days in the coastal regions and the islands. The greater increases of around 25 days were observed all over the country in RCP4.5 in 2075–2099 while the most robust changes were obtained under RCP8.5. More specifically, the regional mean changes increase to 50–60 more days almost all over the country (around 40 days over the mountains) and up to 80 days in the coastal areas of eastern Evia, southwestern Peloponnese, north Crete and the islands. No statistically significant future changes are observed in mountainous areas under both scenarios in the near future period. Hot days (Fig. 18), as characterized by a daily TX larger than 35 °C, have a well-marked increased frequency of 30–45 days, especially for RCP8.5 in the far future, in specific regions such as in the central-eastern mainland (Thessaly region), Thessaloniki region (central Macedonia region), Attica, some areas in Peloponnese, southern Crete and western parts of Greece. No remarkable changes were observed under RCP4.5 during both periods. It is also obvious that the areas with non-statistically significance change is centered only in the mountainous areas of central Greece and Peloponnese in the far future period under RCP8.5.

Regarding the tropical nights number illustrated in Fig. 19, a general increase of about up to 30 days is found under RCP4.5 and RCP8.5 for the near future all over the country compared to the reference period. The change becomes more severe in the far future (30–40 days more) for RCP4.5 in the north-west part of Peloponnese and Crete, surpassing the 50 days under RCP8.5 and over the entire country. Only in the mountainous regions tropical nights are seen to reduce, except of the period 2075–2099 in RCP8.5 (30 days of increase). It is also obvious (Fig. 19a) that coastal areas are more affected than continental parts by increased days of tropical nights. No statistically significant changes are observed only in mountainous areas of central

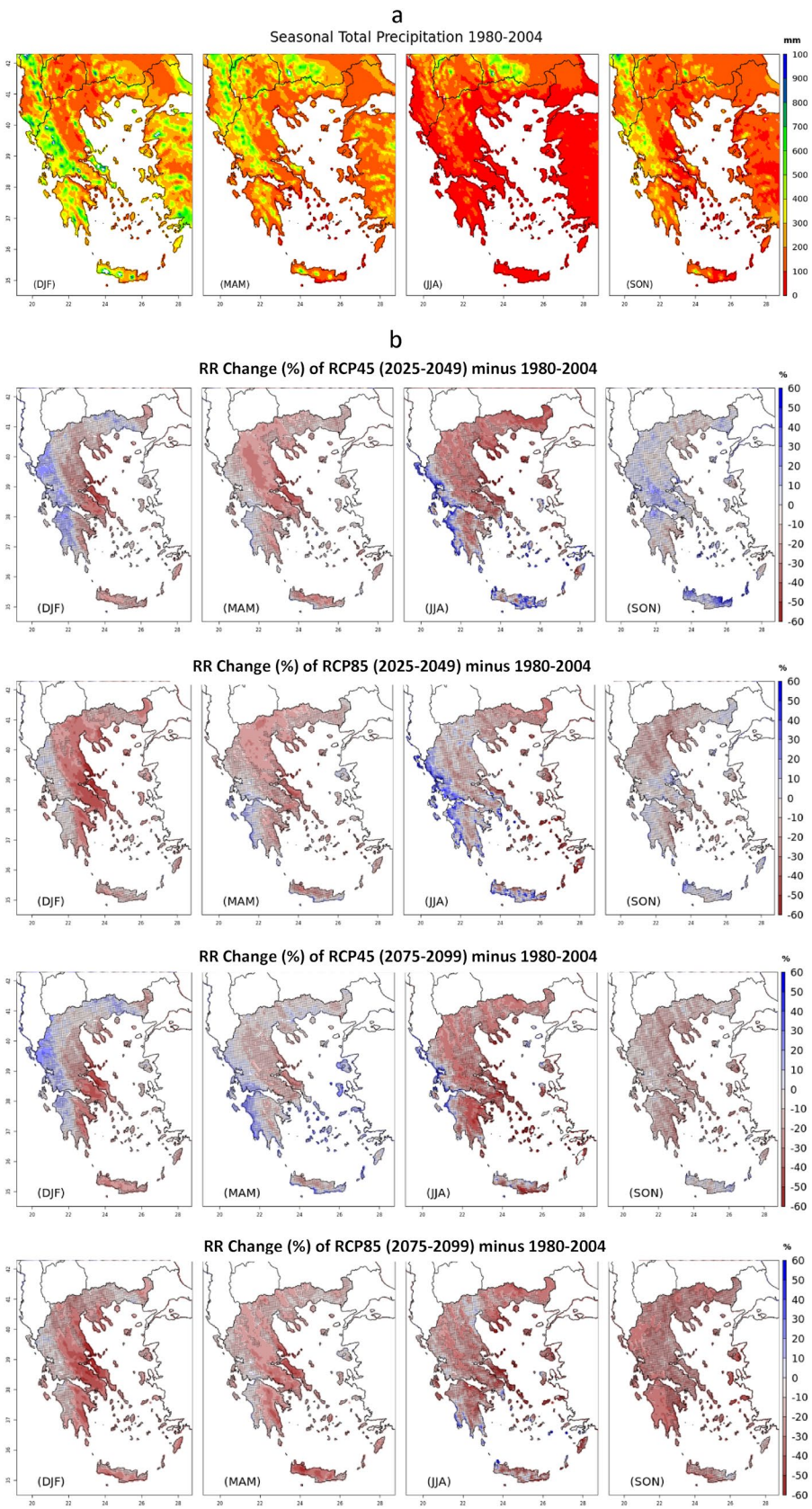

Fig. 15 **a** WRFEC mean historical climatology, **b** Seasonal mean precipitation relative changes given by WRFEC for RCP4.5 and RCP8.5. (Areas with dots specify changes not statistically significant using a Student's t test at the 95% confidence level)

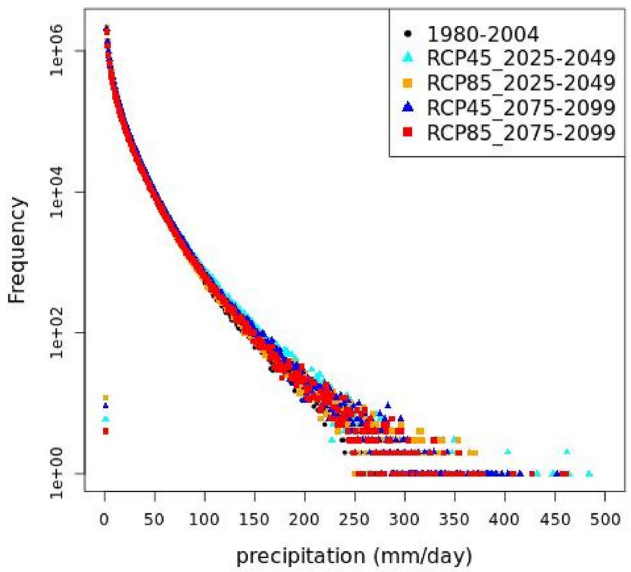

Fig. 16 WRFEC PDFs of precipitation (mm/day) in the historical and future climate periods

Greece and Peloponnese under RCP45 for both periods and under RCP8.5 in the near future.

In Fig. 20, a robust reduction is noted in the climate signal of frost days in the mountains, which reduces towards the coastal areas in the far future period. No noticeable differences are observed under both scenarios in the near future period. The strongest reduction of about 60 days is obtained under RCP8.5 in the far future. The calculated changes in frost days are statistically significant everywhere in the domain.

Both indices, illustrated in Figs. 21 and 22, show an increase in the climate change signal of extreme precipitation events, in the western part of the country for RCP4.5 in both periods and, the near future under RCP8.5 (up to 10 days). On the other hand, the highest decreases in the number of days with heavy precipitation are found mainly over the high mountainous areas of Crete and eastern mainland. This reduction is more pronounced under RCP8.5 in the far future The calculated changes in the number of days with heavy rainfall are statistically significant everywhere in the domain (Fig. 21). However, the changes in the very heavy rainfall events are projected with no statistical significance in the north and eastern parts of the mainland during both periods and scenarios.

In what concerns dry days with daily precipitation less than 1 mm (Fig. 23), it is obvious that during both periods and scenarios the eastern part of the country would experience a consistent increase of dry days from 5 to 15 days. In addition, the strongest positive change is shown under RCP8.5 in the far future, all over the country with the most robust signal in the eastern parts (up to 35 days). Meanwhile, a reduction of dry days is reported up to 10 days, in the western parts of the country, the Ionian and Aegean Islands, Crete and some regions in the northeast mainland, with an exception during 2075–2099 under RCP8.5. The calculated changes in dry days are statistically significant everywhere in the domain.

Consequently, the climate change signal derived from the climate indices of extremes shows that it is clearly obvious that in both scenarios and periods extreme events would become gradually more extreme, reaching their peak in RCP8.5. These results are in good agreement with the studies of (Giannakopoulos et al., 2011; Kostopoulou et al. 2014). Leaver 2018 has also highlighted a considerable increase in the likelihood and occurrence of high temperatures based on ETCCDI climate indices based on EU-CORDEX datasets (0.44°) for the area of Greece. In agreement with our findings, another study using EU-CORDEX results (0.11°) reported future warming in Greece with the number of hot days and tropical nights in a year projected to increase significantly and the number of frost days to decrease, particularly under RCP8.5 (Georgoulias et al 2022). Moreover, our results are consistent with EU-CORDEX hot days results for the areas of Italy and the Balkans (where Greece is included) recently analysed by Coppola et al. (2020) where the number of hot days (> 35 °C) is robustly projected to increase by more than 50 days in the far future. Regarding precipitation, dry days become more frequent under RCP8.5 in the far future all over Greece with the eastern part of the country being highly prone to drought events. All these changes would have important impacts on the agriculture production and human discomfort, as these are typical critical thresholds above which these sectors are affected.

5 Conclusions

In this study, we applied for the first time high resolution downscaling (5-km) with WRF driven by the GCMEC model for the area of Greece and for two different future warming scenarios (RCP4.5 and RCP8.5), with 25-year historical data (1980–2004) and two 25 year future time slices (2025–2049 and 2075–2099), to investigate: (1) the model performance in the historical period compared to observational data; and (2) its contribution to the projected changes of the regional climate, regarding the mean minimum and maximum temperatures and total precipitation. The novelty of this work lies in the production and validation of a new and reliable high-resolution dataset of climate variables and pertinent indices for taking into consideration the complex topography of Greece, aiming to provide driving data for impact assessment models and study the potential climate

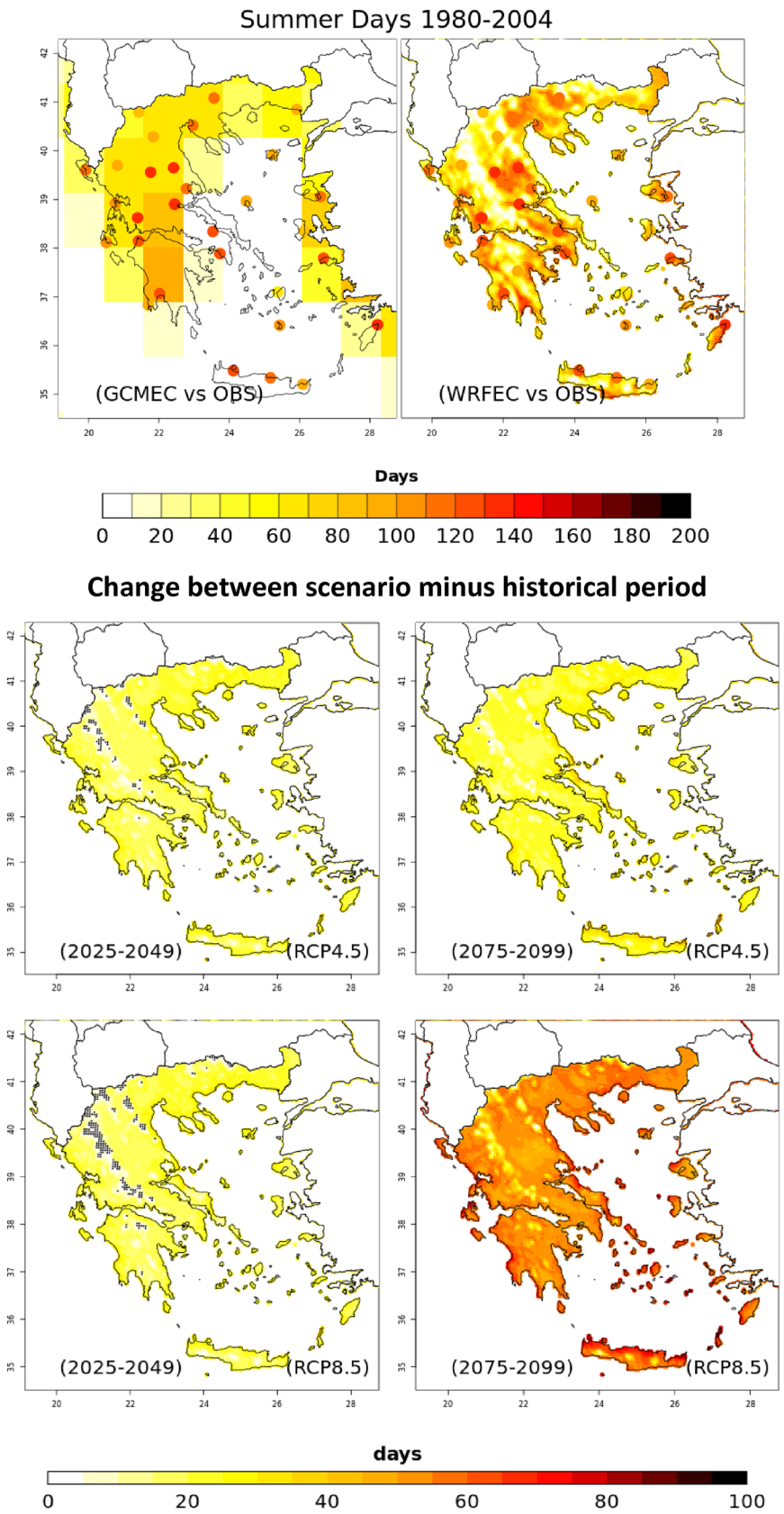

Fig. 17 Annual mean summer days changes for 2025–2049 (near future) and 2075–2099 (far future) relative to 1980–2004. In the top figure, the summer days index is depicted for the historical period. (Areas with dots specify changes not statistically significant using a Student's t-test at the 95% confidence level)

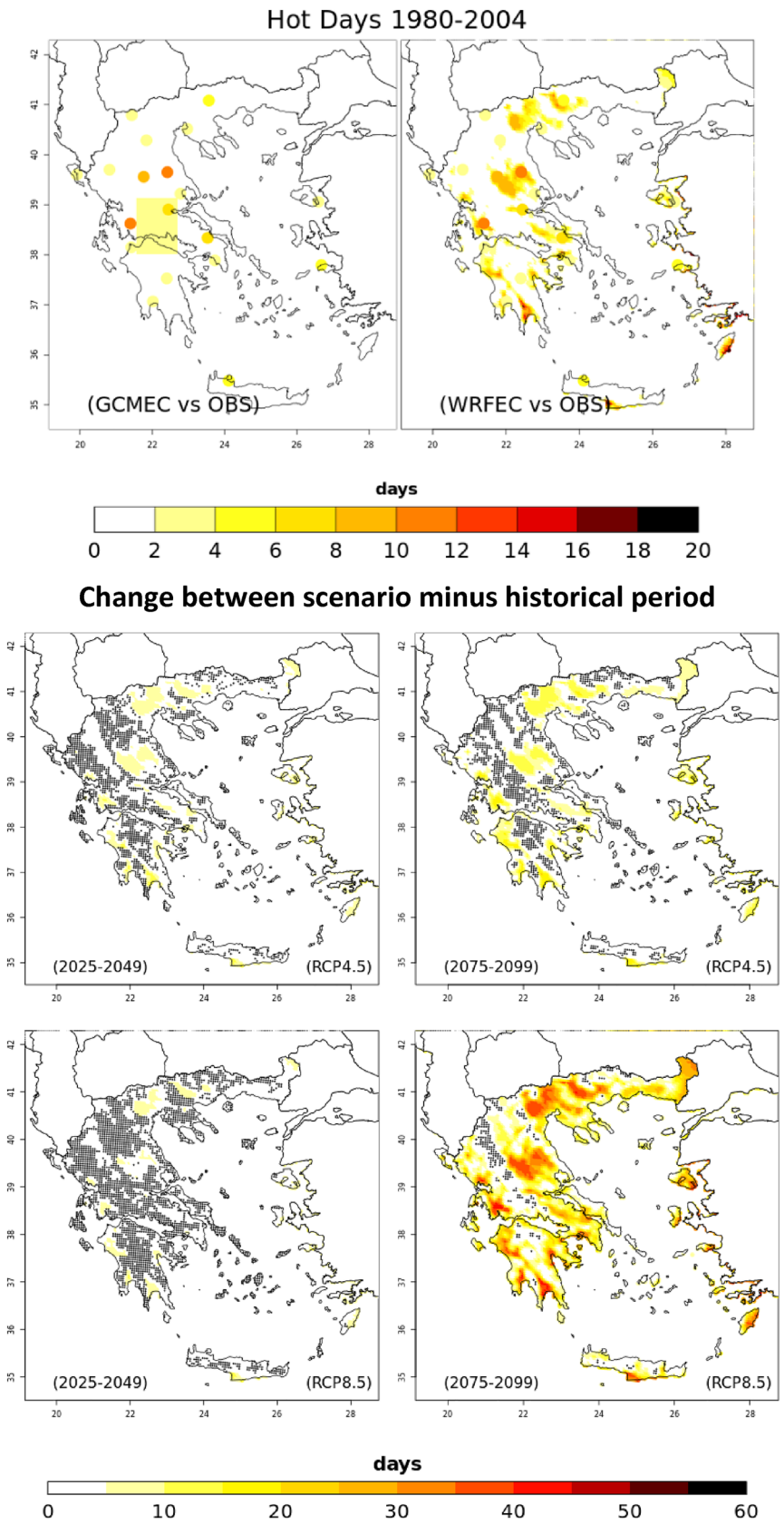

Fig. 18 Annual mean hot days changes for 2025–2049 (near future) and 2075–2099 (far future) relative to 1980–2004. In the top figure, the hot days index is depicted for the historical period. (Areas with dots specify changes not statistically significant using a Student's t-test at the 95% confidence level)

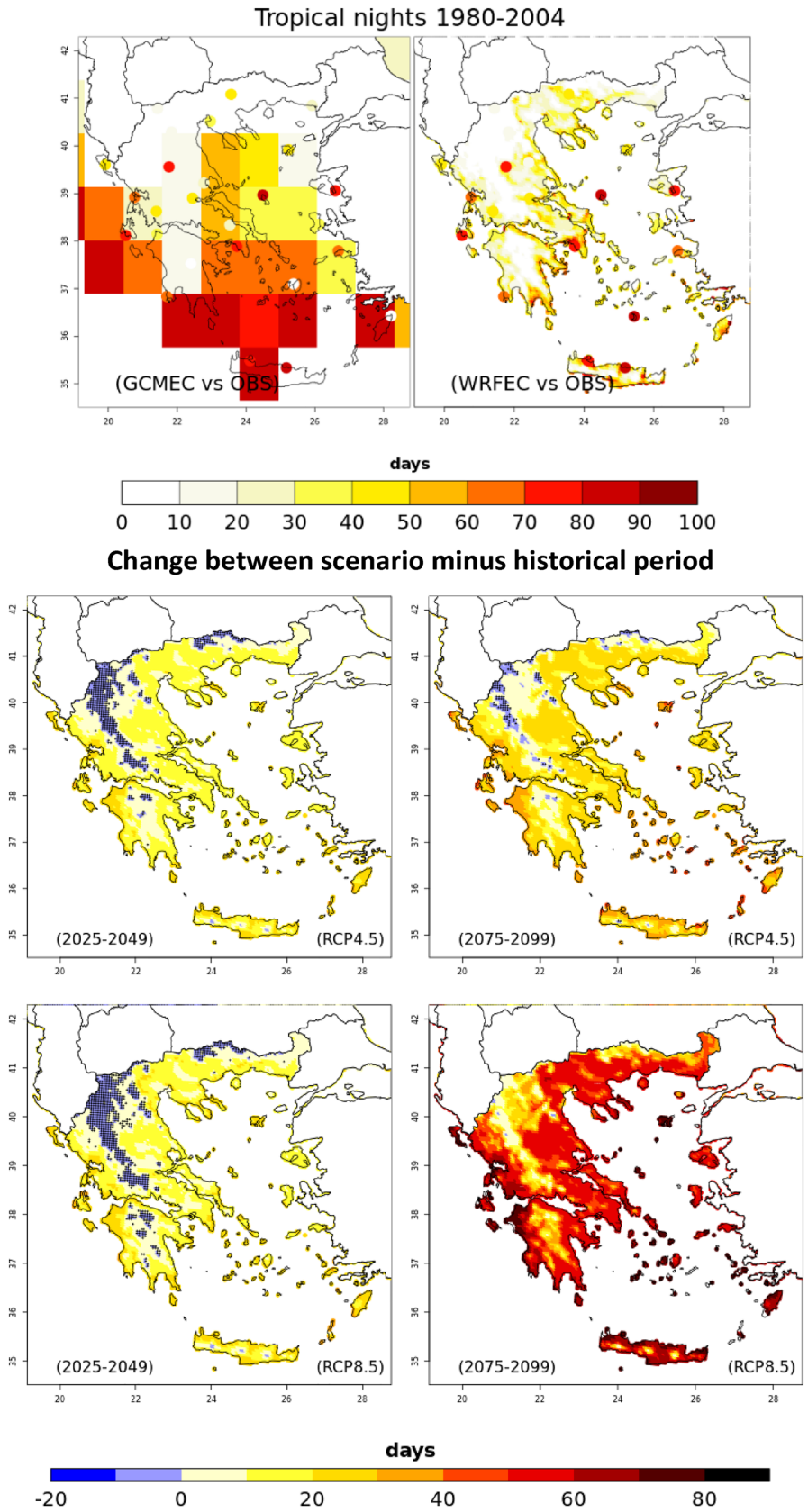

Fig. 19 Annual mean tropical nights changes for 2025–2049 (near future) and 2075–2099 (far future) relative to 1980–2004. In the top figure, the tropical night index is depicted for the historical period. (Areas with dots specify changes not statistically significant using a Student's t-test at the 95% confidence level)

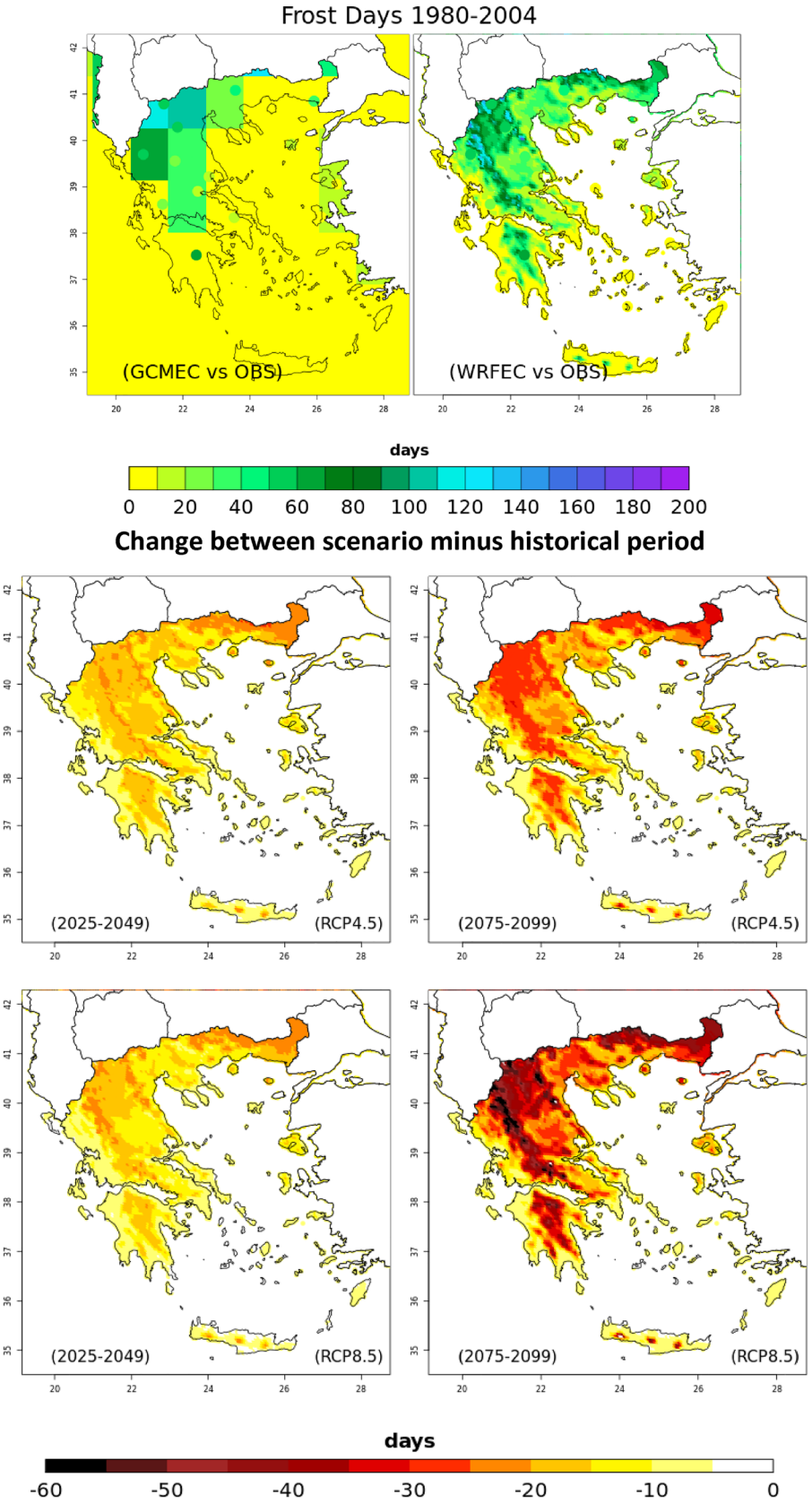

Fig. 20 Annual mean frost days changes for 2025–2049 (near future) and 2075–2099 (near future) relative to 1980- 2004. In the top figure, the frost days index is depicted for the historical period. (Areas with dots specify changes not statistically significant using a Student's t-test at the 95% confidence level)

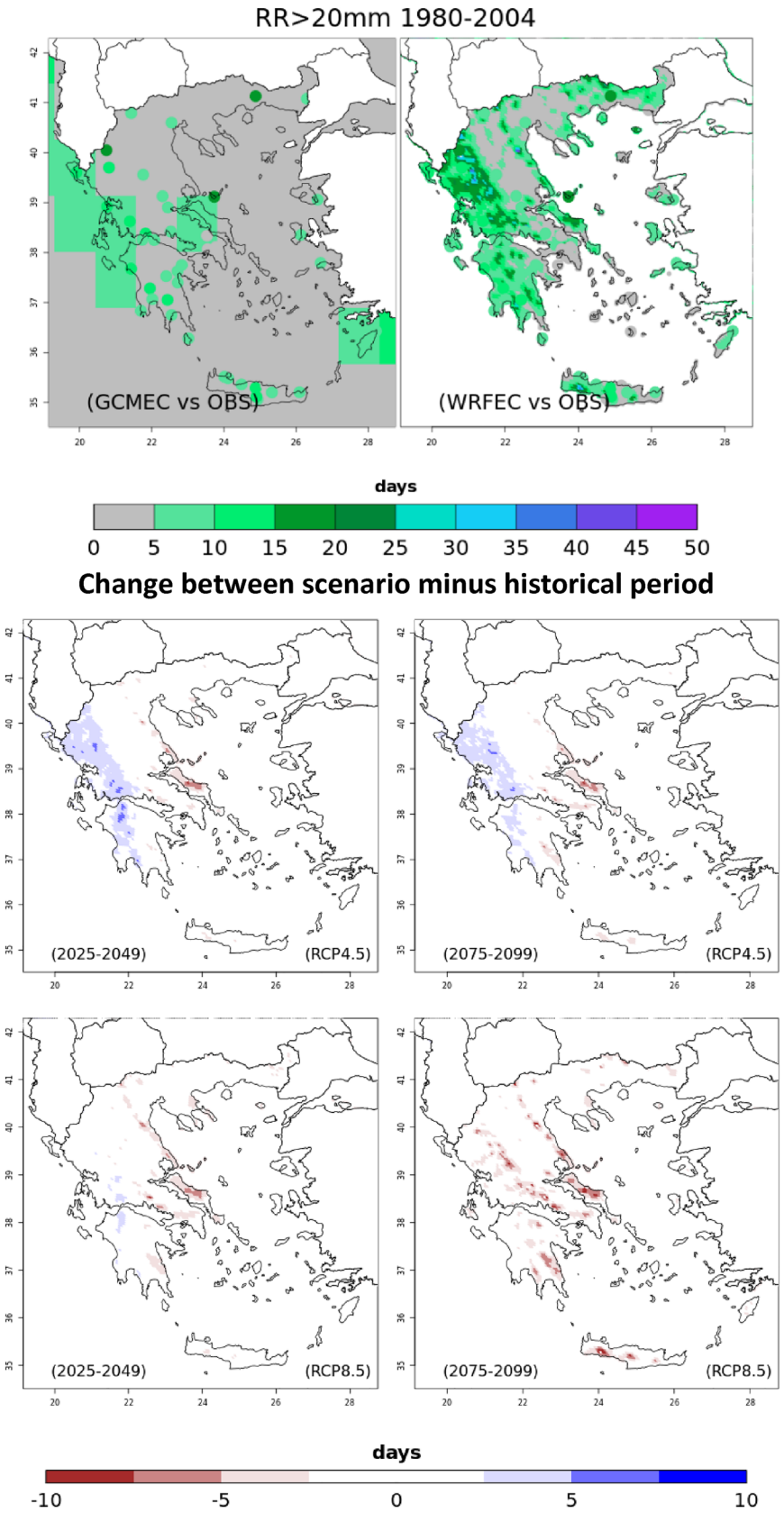

Fig. 21 Annual mean heavy precipitation days changes for 2025–2049 (near future) and 2075–2099 (far future) relative to 1980- 2004. In the top figure, the number of heavy precipitation days (> 20 mm) is depicted for the historical period. (Areas with dots specify changes not statistically significant using a Student's t-test at the 95% confidence level)

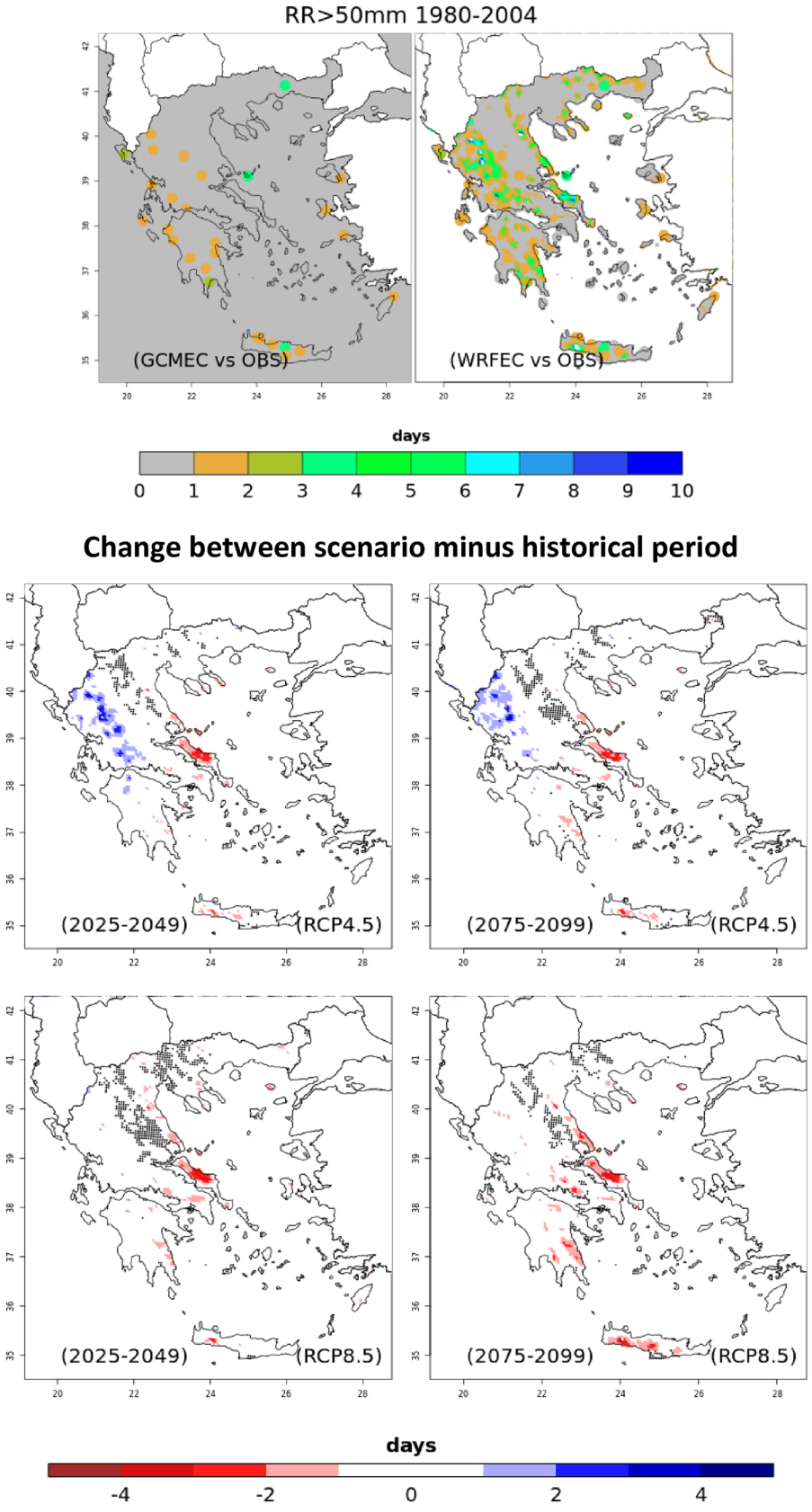

Fig. 22 Annual mean very heavy precipitation days changes for 2025–2049 (near future) and 2075–2099 (far future) relative to 1980–2004. In the top figure, the number of very heavy precipitation days (above 50 mm) is depicted for the historical period. (Areas with dots specify changes not statistically significant using a Student's t-test at the 95% confidence level)

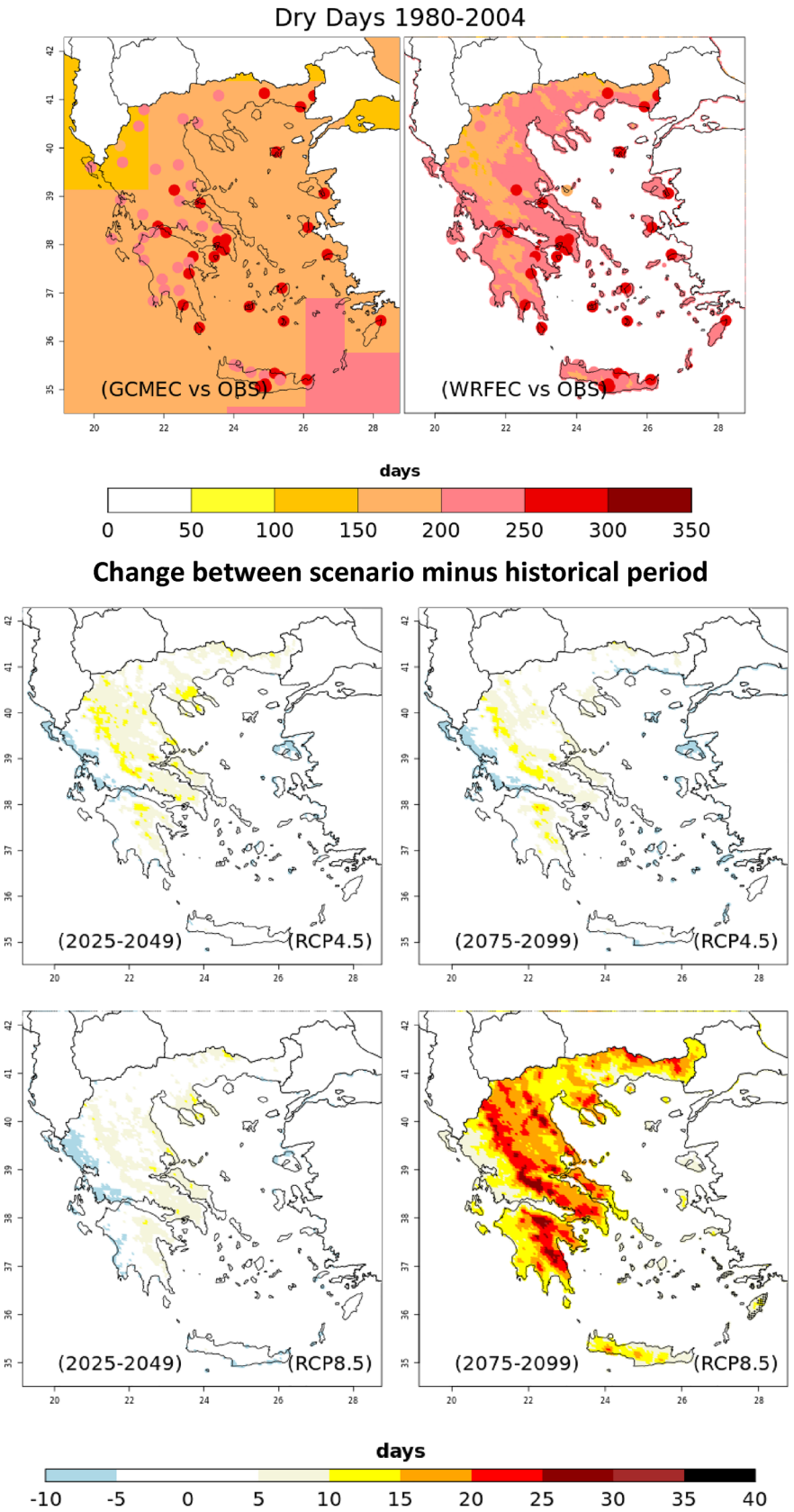

Fig. 23 Annual mean dry days changes for 2025–2049 (near future) and 2075–2099 (far future) relative to 1980- 2004. In the top figure, the number of dry days (below 1 mm) is depicted for the historical period. (Areas with dots specify changes not statistically significant using a Student's t-test at the 95% confidence level)

risks in a region characterized as "climate hot spot" in IPCC AR6 (Ali et al. 2022). We leverage on the added value of the dynamic downscaling process and its outcome to achieve an improved characterization of the expected changes in temperature and precipitation as well as their extremes, an important task in view of the pronounced warming projected in the vulnerable to climatic hazards Mediterranean region.

The model setup driven by reanalysis for downscaling the data in the study area has been extensively evaluated in our previous works in which the results produced reliable climate information compared to available observational datasets. In addition, we have studied the statistical significance of the projected changes. Moreover, we have investigated the performance of the GCM via a statistical evaluation against observations in the reference period to highlight the added value of the downscaled results.

Firstly, the historical model performance evaluation showed that bias results for all temperatures and time scales presented consistent values, with cold bias around 1.1 °C for TX and a warm bias of 0.24 °C for TN with high correlation values with observations during monthly and seasonal time scales. The historical WRFEC generally simulated a dry bias in total precipitation, which was extended to almost the whole country with some excess of precipitation extreme events during spring and summer, but with good description of the spatial precipitation pattern. Overall, those findings suggested that our downscaling method was able to produce results in line with the historical observations.

The EC-EARTH and WRF model evaluations in the historical period was followed by a high-resolution analysis of climate change projections. WRFEC results projected a noticeable magnitude of warming regarding TX with the most pronounced changes up to 5 °C mostly over the eastern parts of the country under the RCP8.5 in the far future period. In addition, the model's projection in summer predicted a larger magnitude (near 5 °C) of warming for TN in the far future over the western part of the mainland, the Ionian Islands, and in some plains of central and northern mainland and southern Crete. The climate change signal of precipitation revealed a general decrease of the annual precipitation all over the eastern part of the country (with islands included) with the most dramatic reductions (above 40%) in seasonal precipitation observed under RCP8.5 almost all over the country in the far future. The model also estimated statistically non-significant changes of increasing rainfall during autumn and spring, of more than 10% in some small areas of western Greece in both periods and RCPs (except of RCP8.5 in the far future).

The projected changes in temperature and precipitation are related to dynamic and thermodynamic future changes. According to Giorgi and Lionello 2008, the drying in the Mediterranean region is associated with increasing anticyclonic circulation which causes a northward shift of the mid-latitude storm track. This northward shift has a seasonal migration and it is maximum in summer and minimum in winter. Lionello and Scarascia 2018 reported that the circulation change would lead to a significant reduction of precipitation for most of the region (Greece included) due to the intensification of the Azores anticyclone in summer that causes increased advection of warm dry continental air masses towards the eastern Mediterranean. The same study concluded that in winter, the increase in barotropic sea level pressure and geopotential height at the 500 hPa level in central Mediterranean hinders the penetration of humid air from the Atlantic towards the southern and eastern Mediterranean areas. Additionally, in the study of a comparative assessment of backward trajectories with WRCEC in the near future and both RCPs, Karozis et al. (2021) deduced for Greece a reduction of cyclones up to 45% originating from the cyclogenesis region of the central Mediterranean and the Adriatic Sea. Moreover, the same study revealed the tendency (higher probability of occurrence) of increased long-range southerly flows from Africa (circa 40%) under RCP4.5 and consequently the appearance of an increased number of heatwaves that could also result in drier conditions in the future. Russo et al. (2014) and Coumou et al. (2018) also reported future enhancement of mid-latitude heat waves due to nonlinear interactions between Arctic teleconnections and other remote and regional feedback processes.

In what concerns the climate change signal derived from ETCCDI indices, the number of summer days is considerable increasing everywhere and particularly under RCP8.5 in the far future. The highest increases of hot days (greater than 35 days of daily TX > 35 °C) are observed over the plains of central-east mainland, central Macedonia, western mainland and Peloponnese under RCP8.5. Our results showed decrease in the number of tropical nights, over the highly mountainous areas of the mainland and Crete in both periods and under both RCPs. On the other hand, their number increased elsewhere, becoming more vivid towards the coastal areas, particularly in the far future under RCP8.5 over the islands and parts of the western mainland. The number of frost days decreases everywhere in both periods and under both RCPs reaching most significant decreases over the mountainous areas and the eastern parts of the mainland under both RCPs in the far future. Regarding precipitation climate indices, our findings revealed a reduction in the number days with RR > 20 mm everywhere apart from western Greece in both periods under RCP4.5 and in the near future under RCP8.5. The increases in the number of days of extreme precipitation (RR > 50 mm) are less profound and mostly over the high altitudes of western Greece in both periods under both RCPs. Yet, the largest decreases are found over the highly mountainous areas of eastern mainland and Crete in the far future and under both RCPs. The number

of dry days decreases in western Greece and the islands in both periods and under both RCPs, with an exception during 2075–2099 under RCP8.5. Significant increases are found over the mountainous areas and eastern mainland, which become more robust in the far future under RCP8.5.

The presented study constituted a first attempt to demonstrate the benefits of a high-resolution dynamical downscaling to simulate as accurately as possible the regional climate and future changes in Greece. Further to this, the study aimed to provide driving data for impact models that require high spatial details. It must be mentioned that at this stage, only one GCM and RCM have been used limiting the quantification of the uncertainty of the results. Also, bias correction was not applied to improve the climate projections regarding the examined variables, given the lack of consistent gridded observational datasets required for such regions of complex topography and climate variation. In summary, uncertainties still exist in projecting future climate changes in Greece—a region with complex topography and unique weather and climate systems, thus, the importance of in-depth analyses of model simulations and large ensembles of high resolution should be emphasized. A natural follow up would also be to investigate the use of an ensemble of different bias corrected methods results with station observational data to quantify the spread of the dynamical downscaling results in the past and future periods for climate indices and particularly for specific areas which are projected to be more affected by extreme events in the future.

Supplementary Information The online version contains supplementary material available at https://doi.org/10.1007/s00382-022-06590-w.

Acknowledgements We acknowledge the data providers in the HNMS. We kindly acknowledge Rita M. Cardoso and Pedro M. M. Soares from the Insituto Dom Luiz of University of Lisbon (Portugal) for providing EC-EARTH model input data and their guidance. This work was supported by computational time granted from the Greek Research and Technology Network (GRNET) in the National HPC facility, ARIS, under projects ID HRCOG (pr004020) and HRPOG (pr006028).

Author contributions Conceptualization: NP, AS and DV; methodology: NP and AS; software: NP; validation: NP; formal analysis: NP; investigation: NP, DV and AS; writing—original draft preparation: NP; writing—review and editing: DV and AS; visualization: NP; supervision: PTN, DV and AS. All authors read and approved the final manuscript.

Funding Open access funding provided by HEAL-Link Greece. Partly funded by EU H2020 FirEUrisk "Developing A Holistic, Risk-Wise Strategy for European Wildfire Management" GA 101003890.

Availability of data and material The datasets generated during the current study are not publicly available due to size and space limitations but are available from the corresponding author on reasonable request.

Code availability Not applicable.

Declarations

Conflict of interest The authors declare no conflict of interest.

References

Ali E, Cramer W, Carnicer J et al (2022) Cross-chapter paper 4: Mediterranean region. In: Pörtner H-O, Roberts DC, Tignor M, Poloczanska ES, Mintenbeck K, Alegría A, Craig M, Langsdorf S, Löschke S, Möller V, Okem A, Rama B (eds) Climate change 2022: impacts, adaptation, and vulnerability. Contribution of working group II to the sixth assessment report of the intergovernmental panel on climate change. Cambridge University Press, Cambridge **(in press)**

Anagnostopoulou C (2017) Future drought projection for the Greek region. Bull Geol Soc Greece 50:1038. https://doi.org/10.12681/bgsg.11808

Ban N, Caillaud C, Coppola E et al (2021) The first multi-model ensemble of regional climate simulations at kilometer-scale resolution, part I: evaluation of precipitation. Clim Dyn 57:275–302. https://doi.org/10.1007/S00382-021-05708-W

Barcikowska MJ, Kapnick SB, Feser F (2018) Impact of large-scale circulation changes in the North Atlantic sector on the current and future Mediterranean winter hydroclimate. Clim Dyn 50:2039–2059. https://doi.org/10.1007/s00382-017-3735-5

Barros V (ed) (2014) Climate change 2014: impacts, adaptation, and vulnerability. part b: regional aspects. contribution of working group ii to the fifth assessment. Cambridge University Press

Barstad I, Sorteberg A, Flatøy F, Déqué M (2009) Precipitation, temperature and wind in Norway: dynamical downscaling of ERA40. Clim Dyn 33:769–776. https://doi.org/10.1007/s00382-008-0476-5

Basharin D, Polonsky A, Stankūnavičius G (2015) Projected precipitation and air temperature over Europe using a performance-based selection method of CMIP5 GCMs. J Water Clim Change 7:103–113. https://doi.org/10.2166/wcc.2015.081

Berg P, Wagner S, Kunstmann H, Schädler G (2013) High resolution regional climate model simulations for Germany: part I—validation. Clim Dyn 40:401–414. https://doi.org/10.1007/s00382-012-1508-8

Cardoso RM, Soares PMM, Lima DCA, Miranda PMA (2019) Mean and extreme temperatures in a warming climate: EURO CORDEX and WRF regional climate high-resolution projections for Portugal. Clim Dyn 52:129–157. https://doi.org/10.1007/s00382-018-4124-4

Cardoso RM, Soares PMM, Miranda PMA, Belo-Pereira M (2013) WRF high resolution simulation of Iberian mean and extreme precipitation climate. Int J Climatol 33:2591–2608. https://doi.org/10.1002/joc.3616

Cattiaux J, Douville H, Peings Y (2013) European temperatures in CMIP5: origins of present-day biases and future uncertainties. Clim Dyn 41:2889–2907. https://doi.org/10.1007/S00382-013-1731-Y/FIGURES/12

Chen N, Gao X, Nan C, Xuejie G (2019) Climate change in the twenty-first century over China: projections by an RCM and the driving GCM. New Publ Keai 12:270–277. https://doi.org/10.1080/16742834.2019.1612695

Coppola E, Nogherotto R, Ciarlo' JM, et al (2021) Assessment of the European climate projections as simulated by the large EURO-CORDEX regional and global climate model ensemble. J Geophys Res Atmos 126:e2019JD032356. https://doi.org/10.1029/2019JD032356

Coppola E, Sobolowski S, Pichelli E et al (2020) A first-of-its-kind multi-model convection permitting ensemble for investigating convective phenomena over Europe and the Mediterranean. Clim Dyn 55:3–34. https://doi.org/10.1007/s00382-018-4521-8

Coumou D, di Capua G, Vavrus S et al (2018) The influence of Arctic amplification on mid-latitude summer circulation. Nat Commun 9:1–12. https://doi.org/10.1038/s41467-018-05256-8

Dasari HP, Salgado R, Perdigao J, Challa VS (2014) A regional climate simulation study using WRF-ARW model over Europe and evaluation for extreme temperature weather events. Int J Atmos Sci 2014:1–22. https://doi.org/10.1155/2014/704079

Diffenbaugh NS, Giorgi F (2012) Climate change hotspots in the CMIP5 global climate model ensemble. Clim Change 114:813–822. https://doi.org/10.1007/S10584-012-0570-X/FIGURES/6

Droutsa KG, Kontoyiannidis S, Balaras CA et al (2021) Climate change scenarios and their implications on the energy performance of hellenic non-residential buildings. Sustainability 13:13005. https://doi.org/10.3390/SU132313005

Eleftheriou D, Kiachidis K, Kalmintzis G et al (2018) Determination of annual and seasonal daytime and nighttime trends of MODIS LST over Greece—climate change implications. Sci Total Environ 616–617:937–947. https://doi.org/10.1016/j.scitotenv.2017.10.226

European Environment Information and Observation Network (Eionet) (2022) Global and European temperatures. https://www.eea.europa.eu/ims/global-and-european-temperatures. Accessed 24 June 2022

Feyen L, Ciscar JC, Gosling S et al (2020) JRC science for policy report JRC PESETA IV final report

Forster PM, Maycock AC, McKenna CM, Smith CJ (2019) Latest climate models confirm need for urgent mitigation. Nat Clim Change 10:7–10. https://doi.org/10.1038/s41558-019-0660-0

Gao Y, Xu J, Chen D (2015) Evaluation of WRF mesoscale climate simulations over the Tibetan Plateau during 1979–2011. J Clim 28:2823–2841. https://doi.org/10.1175/JCLI-D-14-00300.1

García-Valdecasas Ojeda M, Raquel Gámiz-Fortis S, Manuel Hidalgo-Muñoz J et al (2015) Regional climate model sensitivity to different parameterizations schemes with WRF over Spain. Geophys Res Abstr EGU Gen Assem 17:2015–11640

Garrido JL, González-Rouco JF, Vivanco MG, Navarro J (2020) Regional surface temperature simulations over the Iberian Peninsula: evaluation and climate projections. Clim Dyn 55:3445–3468. https://doi.org/10.1007/s00382-020-05456-3

Georgoulias AK, Akritidis D, Kalisoras A et al (2022) Climate change projections for Greece in the 21st century from high-resolution EURO-CORDEX RCM simulations. Atmos Res. https://doi.org/10.1016/j.atmosres.2022.106049

Giannakopoulos C, Kostopoulou E, Varotsos KV et al (2011) An integrated assessment of climate change impacts for Greece in the near future. Reg Environ Change 11:829–843. https://doi.org/10.1007/S10113-011-0219-8/TABLES/5

Giorgi F (2006) Climate change hot-spots. Geophys Res Lett 33:L08707. https://doi.org/10.1029/2006GL025734

Giorgi F, Bi X, Pal J (2004) Mean, interannual variability and trends in a regional climate change experiment over Europe. II: climate change scenarios (2071–2100). Clim Dyn 23:839–858. https://doi.org/10.1007/S00382-004-0467-0/FIGURES/14

Giorgi F, Hewitson B, Christensen J et al (2001) Regional climate information evaluation and projections. Climate Change 2001: the scientific basis contribution of working group I to the third assessment report of the intergovernmental panel on climate change

Giorgi F, Lionello P (2008) Climate change projections for the Mediterranean region. Glob Planet Change 63:90–104. https://doi.org/10.1016/j.gloplacha.2007.09.005

Hatzianastassiou N, Katsoulis B, Pnevmatikos J, Antakis V (2008) Spatial and temporal variation of precipitation in Greece and surrounding regions based on global precipitation climatology project data. J Clim 21:1349–1370. https://doi.org/10.1175/2007JCLI1682.1

Hawkins E, Sutton R (2009) The potential to narrow uncertainty in regional climate predictions. Bull Am Meteorol Soc 90:1095–1107. https://doi.org/10.1175/2009BAMS2607.1

Hay LE, Wilby RL, Leavesley GH (2000) A comparison of delta change and downscaled GCM scenarios for three mountainous basins in the United States. J Am Water Resour Assoc 36:387–397

Hazeleger W, Severijns C, Semmler T et al (2010) EC-Earth: a seamless earth-system prediction approach in action. Bull Am Meteorol Soc 91:1357–1364. https://doi.org/10.1175/2010BAMS2877.1

Hazeleger W, Wouters B, van Oldenborgh GJ et al (2013) Predicting multiyear North Atlantic Ocean variability. J Geophys Res Oceans 118:1087–1098. https://doi.org/10.1002/JGRC.20117

Heikkilä U, Sandvik A, Sorteberg A (2011) Dynamical downscaling of ERA-40 in complex terrain using the WRF regional climate model. Clim Dyn 37:1551–1564. https://doi.org/10.1007/s00382-010-0928-6

Hofstra N, New M, McSweeney C (2010) The influence of interpolation and station network density on the distributions and trends of climate variables in gridded daily data. Clim Dyn 35:841–858. https://doi.org/10.1007/s00382-009-0698-1

Iacono MJ, Delamere JS, Mlawer EJ et al (2008) Radiative forcing by long-lived greenhouse gases: calculations with the AER radiative transfer models. J Geophys Res 113:D13103. https://doi.org/10.1029/2008JD009944

Jacob D, Petersen J, Eggert B et al (2014) EURO-CORDEX: new high-resolution climate change projections for European impact research. Reg Environ Change 14:563–578. https://doi.org/10.1007/s10113-013-0499-2

Jacob D, Teichmann C, Sobolowski S et al (2020) Regional climate downscaling over Europe: perspectives from the EURO-CORDEX community. Reg Environ Change 20:1–20. https://doi.org/10.1007/S10113-020-01606-9/FIGURES/3

Janjić ZI (2001) Nonsingular implementation of the Mellor-Yamada level 2.5 scheme in the NCEP Meso model

Kairis O, Karamanos A, Voloudakis D et al (2022) Identifying degraded and sensitive to desertification agricultural soils in Thessaly, Greece, under simulated future climate scenarios. Land (basel) 11:395. https://doi.org/10.3390/land11030395

Karozis S, Sfetsos A, Gounaris N, Vlachogiannis D (2021) An assessment of climate change impact on air masses arriving in Athens, Greece. Theor Appl Climatol 145:501–517. https://doi.org/10.1007/S00704-021-03624-X

Katavoutas G, Founda D, Kitsara G, Giannakopoulos C (2021) Climate change and thermal comfort in top tourist destinations—the case of Santorini (Greece). Sustainability 13:9107. https://doi.org/10.3390/SU13169107

Katopodis T, Markantonis I, Politi N et al (2020) High-resolution solar climate atlas for greece under climate change using the weather research and forecasting (WRF) model. Atmosphere (basel). https://doi.org/10.3390/ATMOS11070761

Katopodis T, Markantonis I, Vlachogiannis D et al (2021) Assessing climate change impacts on wind characteristics in Greece through high resolution regional climate modelling. Renew Energy 179:427–444. https://doi.org/10.1016/j.renene.2021.07.061

Katopodis T, Vlachogiannis D, Politi N et al (2019) Assessment of climate change impacts on wind resource characteristics and wind energy potential in Greece. J Renew Sustain Energy 11:066502. https://doi.org/10.1063/1.5118878

Knist S, Goergen K, Simmer C (2020) Evaluation and projected changes of precipitation statistics in convection-permitting WRF climate simulations over Central Europe. Clim Dyn 55:325–341. https://doi.org/10.1007/s00382-018-4147-x

Komurcu M, Emanuel KA, Huber M, Acosta RP (2018) High-resolution climate projections for the northeastern United States using dynamical downscaling at convection-permitting scales. Earth Space Sci 5:801–826. https://doi.org/10.1029/2018EA000426

Kostopoulou E, Giannakopoulos C, Hatzaki M et al (2014) Spatio-temporal patterns of recent and future climate extremes in the eastern Mediterranean and Middle East region. Nat Hazard 14:1565–1577. https://doi.org/10.5194/nhess-14-1565-2014

Kotlarski S, Keuler K, Christensen OB et al (2014) Regional climate modeling on European scales: a joint standard evaluation of the EURO-CORDEX RCM ensemble. Geosci Model Dev 7:1297–1333. https://doi.org/10.5194/gmd-7-1297-2014

Kryza M, Wałaszek K, Ojrzyńska H et al (2017) High-resolution dynamical downscaling of ERA-interim using the WRF regional climate model for the area of Poland. Part 1: model configuration and statistical evaluation for the 1981–2010 period. Pure Appl Geophys 174:511–526. https://doi.org/10.1007/s00024-016-1272-5

Leaver J (2018) A climate impact assessment for the future of Greece and its adaptation capacity as influenced by socio-economic factor

Lionello P, Scarascia L (2018) The relation between climate change in the Mediterranean region and global warming. Reg Environ Change 18:1481–1493. https://doi.org/10.1007/s10113-018-1290-1

Lyra A, Tavares P, Chou SC et al (2018) Climate change projections over three metropolitan regions in Southeast Brazil using the non-hydrostatic Eta regional climate model at 5-km resolution. Theor Appl Climatol 132:663–682. https://doi.org/10.1007/s00704-017-2067-z

Maheras P, Kostopoulou E, Tolika K, Tegoulias I, Giannakopoulos C and Anagnostopoulou C (2008) Evaluation of a regional climate model over the Balkan Peninsula. In: 9th Panellenic conference of meteorology and climatology. Thessaloniki, Greece

Mariotti A, Dell'Aquila A (2012) Decadal climate variability in the Mediterranean region: roles of large-scale forcings and regional processes. Clim Dyn 38:1129–1145. https://doi.org/10.1007/S00382-011-1056-7/FIGURES/10

Mellor GL, Yamada T (1982) Development of a turbulence closure model for geophysical fluid problems. Rev Geophys 20:851. https://doi.org/10.1029/RG020i004p00851

Moss RH, Edmonds JA, Hibbard KA et al (2010) The next generation of scenarios for climate change research and assessment. Nature 463:747–756. https://doi.org/10.1038/nature08823

Nakicenovic N, Alcamo J, Grubler A et al (2000) Special report on emissions scenarios (SRES), a special report of working group III of the intergovernmental panel on climate change

Nastos PT, Matzarakis A (2019) Present and future climate—tourism conditions in Milos Island, Greece. Atmosphere 10:145. https://doi.org/10.3390/ATMOS10030145

Pérez JC, Díaz JP, González A et al (2014) Evaluation of WRF parameterizations for dynamical downscaling in the Canary Islands. J Clim 27:5611–5631. https://doi.org/10.1175/JCLI-D-13-00458.1

Politi N, Nastos PT, Sfetsos A et al (2017) Comparison and validation of WRF model physics parameterizations over the domain of Greece. Perspectives on atmospheric sciences. Springer, Cham, pp 55–61

Politi N, Nastos PT, Sfetsos A et al (2018) Evaluation of the AWR-WRF model configuration at high resolution over the domain of Greece. Atmos Res. https://doi.org/10.1016/J.ATMOSRES.2017.10.019

Politi N, Sfetsos A, Vlachogiannis D et al (2020) A sensitivity study of high-resolution climate simulations for Greece. Climate 8:1–28. https://doi.org/10.3390/cli8030044

Politi N, Vlachogiannis D, Sfetsos A, Nastos PT (2021) High-resolution dynamical downscaling of ERA-Interim temperature and precipitation using WRF model for Greece. Clim Dyn 57:799–825. https://doi.org/10.1007/S00382-021-05741-9

Prein AF, Gobiet A, Truhetz H et al (2016) Precipitation in the EURO-CORDEX 0.11° and 0.44° simulations: high resolution, high benefits. Clim Dyn 46:383–412. https://doi.org/10.1007/s00382-015-2589-y

Riahi K, Rao S, Krey V et al (2011) RCP 8.5—a scenario of comparatively high greenhouse gas emissions. Clim Change 109:33–57. https://doi.org/10.1007/S10584-011-0149-Y/FIGURES/12

Rovithakis A, Grillakis MG, Seiradakis KD et al (2022) Future climate change impact on wildfire danger over the Mediterranean: the case of Greece. Environ Res Lett 17:045022. https://doi.org/10.1088/1748-9326/AC5F94

Russo S, Dosio A, Graversen RG et al (2014) Magnitude of extreme heat waves in present climate and their projection in a warming world. J Geophys Res Atmos 119:12500–12512. https://doi.org/10.1002/2014JD022098

Skamarock WC, Skamarock WC, Klemp JB, et al (2008) A description of the advanced research WRF version 3. NCAR Technical note -475+STR

Soares PMM, Cardoso RM (2018) A simple method to assess the added value using high-resolution climate distributions: application to the EURO-CORDEX daily precipitation. Int J Climatol 38:1484–1498. https://doi.org/10.1002/JOC.5261

Soares PMM, Cardoso RM, Lima DCA, Miranda PMA (2017) Future precipitation in Portugal: high-resolution projections using WRF model and EURO-CORDEX multi-model ensembles. Clim Dyn 49:2503–2530. https://doi.org/10.1007/s00382-016-3455-2

Soares PMM, Cardoso RM, Miranda PMA et al (2012) WRF high resolution dynamical downscaling of ERA-interim for Portugal. Clim Dyn 39:2497–2522. https://doi.org/10.1007/s00382-012-1315-2

Sun X, Xue M, Brotzge J et al (2016) An evaluation of dynamical downscaling of Central Plains summer precipitation using a WRF-based regional climate model at a convection-permitting 4 km resolution. J Geophys Res Atmos 121:13801–813825. https://doi.org/10.1002/2016JD024796

Sylla MB, Gaye AT, Pal JS et al (2009) High-resolution simulations of West African climate using regional climate model (RegCM3) with different lateral boundary conditions. Theor Appl Climatol 98:293–314. https://doi.org/10.1007/s00704-009-0110-4

Tian L, Jin J, Wu P et al (2020) High-resolution simulations of mean and extreme precipitation with WRF for the soil-erosive Loess Plateau. Clim Dyn 54:3489–3506. https://doi.org/10.1007/s00382-020-05178-6

Tolika CK, Zanis P (2012) Regional climate change scenarios for Greece: future temperature and precipitation projections from ensembles of RCMs. Glob NEST J 14:407–421

Torma C, Giorgi F, Coppola E (2015) Added value of regional climate modeling over areas characterized by complex terrain-precipitation over the Alps. J Geophys Res 120:3957–3972. https://doi.org/10.1002/2014JD022781

van der Schriek T, Varotsos KV, Giannakopoulos C, Founda D (2020) Projected future temporal trends of two different urban heat islands in Athens (Greece) under three climate change scenarios:

a statistical approach. Atmosphere 11:637.https://doi.org/10.3390/ATMOS11060637

Varela V, Vlachogiannis D, Sfetsos A et al (2020) Methodology for the study of near-future changes of fire weather patterns with emphasis on archaeological and protected touristic areas in Greece. Forests. https://doi.org/10.3390/f11111168

Varotsos KV, Karali A, Kitsara G, Giannakopoulos C (2021a) Climate change impacts on the Greek tourism sector. EMS2021. https://doi.org/10.5194/EMS2021-324

Varotsos KV, Karali A, Lemesios G et al (2021b) Near future climate change projections with implications for the agricultural sector of three major Mediterranean islands. Reg Environ Change 21:16. https://doi.org/10.1007/s10113-020-01736-0

Vautard R, Kadygrov N, Iles C et al (2021) Evaluation of the large EURO-CORDEX regional climate model ensemble. J Geophys Res Atmos 126:e2019JD032344. https://doi.org/10.1029/2019JD032344

Wagner S, Berg P, Schädler G, Kunstmann H (2013) High resolution regional climate model simulations for Germany: Part II—projected climate changes. Clim Dyn 40:415–427. https://doi.org/10.1007/s00382-012-1510-1

Warrach-Sagi K, Schwitalla T, Wulfmeyer V, Bauer HS (2013) Evaluation of a climate simulation in Europe based on the WRF-NOAH model system: precipitation in Germany. Clim Dyn 41:755–774. https://doi.org/10.1007/s00382-013-1727-7

Warscher M, Wagner S, Marke T et al (2019) A 5 km resolution regional climate simulation for Central Europe: performance in high mountain areas and seasonal, regional and elevation-dependent variations. Atmosphere (Basel). https://doi.org/10.3390/atmos10110682

Zelinka MD, Myers TA, McCoy DT et al (2020) Causes of higher climate sensitivity in CMIP6 models. Geophys Res Lett 47:e2019GL085782. https://doi.org/10.1029/2019GL085782

Zerefos CS, Repapis C, Giannakopoulos C et al (2011) The climate of the Eastern Mediterranean and Greece: past, present and future. The environmental, economic and social impacts of climate change in Greece, pp 1–126

Zittis G, Hadjinicolaou P, Klangidou M et al (2019) A multi-model, multi-scenario, and multi-domain analysis of regional climate projections for the Mediterranean. Reg Environ Change 19:2621–2635. https://doi.org/10.1007/S10113-019-01565-W/FIGURES/6